CONF-8609383--

AMERICAN COLLEGE OF NUCLEAR PHYSICIANS
AND
THE SOCIETY OF NUCLEAR MEDICINE

CLINICAL SPECT SYMPOSIUM

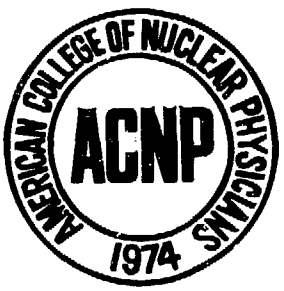

SNM

The Washington Marriott Hotel
September 22-23, 1986
Washington, D.C.

Bm 1-6-88

CONF-8609383--

DE88 003984

Proceedings of

CLINICAL SPECT SYMPOSIUM

SEPTEMBER 1986

Co-sponsored by

AMERICAN COLLEGE OF NUCLEAR PHYSICIANS

and

SOCIETY OF NUCLEAR MEDICINE

This program is being sponsored by a grant from

THE DEPARTMENT OF ENERGY

OFFICE OF HEALTH & ENVIRONMENTAL RESEARCH

Contributors

NATIONAL CANCER INSTITUTE/NIH

CENTER FOR DEVICE CONTROL/FDA

American College of Nuclear Physicians
1986-6

SPECT IN CLINICAL PRACTICE

MONDAY - SEPTEMBER 22, 1986

Table of Contents

8:30-8:45	Introduction - William D. Kaplan, M.D.	1
8:45-9:15	SPECT Imaging: How It Fits Clinically Robert E. Henkin, M.D.	6
9:15-9:45	Review of Current Instrumentation - Robert T. Anger, M.S.	16
10:30-11:00	Understanding Algorithms - Bernard E. Oppenheim, M.D.	23
11:00-11:30	Looking at Things a Different Way: Filtering and Backprojection - Ernest V. Garcia, Ph.D.	27
11:30-12:00	Effects of Attenuation in SPECT - Stephen C. Moore, Ph.D.	34
2:00-2:30	Uniformity Requirements in SPECT - Gerd Muehllehner, Ph.D.	42
2:30-3:00	Clinicians Guide to Technical Artifacts - John W. Keyes, M.D.	44
3:45-4:15	Practical Aspects of Quality Assurance - Robert E. Henkin, M.D.	46
4:15-4:30	Summation - Bernard E. Oppenheim, M.D.	52

SPECT IN CLINICAL PRACTICE

TUESDAY - SEPTEMBER 23, 1986

Table of Contents

8:30-9:00	Patient Set-up for SPECT - Barbara Y. Croft, Ph.D.	54
9:00-9:30	Current Advances in Hepatic SPECT Imaging - Ronald L. Van Heertum, M.D.	58
9:30-10:00	Qualitative and Quantitative Hepatic SPECT Imaging - Harvey A. Ziessman, M.D.	66
10:45-11:15	Functional Brain Imaging with Perfusion Tracers - Thomas C. Hill, M.D.	72
11:15-11:45	Dynamic Brain Imaging with SPECT - Michael D. Devous, Sr., Ph.D.	88
1:30-2:00	SPECT in the Quantitative Imaging of Radiolabeled Antibodies - Peter Leichner, Ph.D.	98
2:00-2:30	SPECT Imaging of the Thorax: Emphasis on Ga-67 for Tumor and Infection - Naomi P. Alazraki, M.D.	102
3:15-3:45	Orthopedic Applications of SPECT Imaging - B. David Collier, M.D.	114
3:45-4:15	SPECT Studies of the Heart - Harvey J. Berger, M.D.	123
4:15-4:45	SPECT-Tl-201 Cardiac Imaging - Daniel S. Berman, M.D.	136
5:00-5:15	Summation - Barbara Y. Croft, Ph.D.	139

SPECT IN CLINICAL PRACTICE

Introduction

William D. Kaplan, M.D.

It has been five years since the last in-depth American College of Nuclear Physicians/Society of Nuclear Medicine Symposium on the subject of single photon emission computed tomography (SPECT) was held. At that time, SPECT was just emerging as a clinical modality, commercial instrumentation was in the developmental stages, routine clinical applications were limited to one or two organ systems, and diagnostic experience were limited to mainly academic centers.

Based upon the results of annual surveys conducted at the 31st and 32nd (1984, 1985) Annual Meeting of the Society of Nuclear Medicine where this subject was nominated as the single most desired topic we have selected SPECT imaging as the basis for this year's program.

From our survey, the most commonly asked question from clinicians initiating SPECT imaging in their clinical laboratories were:

(1) What unique information is available from SPECT studies?

(2) How can I best integrate SPECT studies into my clinical case load?

(3) What commercial equipment is currently available?

(4) What are the technical pitfalls in SPECT acquisition?

The objectives of this symposium, therefore, are to survey the progress of SPECT clinical applications that have taken place over the last five years and to provide practical and timely guidelines to users of SPECT so that this exciting imaging modality can be fully integrated into the evaluation of pathologic processes.

We have divided the program into two broad areas with the first half devoted to a consideration of technical factors important in SPECT acquisition and the second half devoted to those organ systems about which sufficient clinical SPECT imaging data are available.

With respect to the technical aspect of the program we have selected the key areas which demand awareness and attention in order to make SPECT operational in clinical practice. These include selection of equipment, details of uniformity correction, utilization of phantoms for equipment acceptance and quality assurance, the major aspect of algorithms, an understanding of filtered back projection and appropriate choice of filters and an awareness of the most commonly generated artifacts and how to recognize them. Sufficient time has been allowed for question and answer periods so that members of the audience can address specific problem areas.

With respect to the acquisition and interpretation of organ images, the faculty will present information on the major aspects of hepatic, brain, cardiac, skeletal, and immunologic imaging techniques. During each of the presentations, special emphasis will be placed upon currently available radionuclides and every effort will be made to underscore the practical, clinically relevant, and currently achievable techniques of organ imaging.

After attending this symposium, participants should be able to list the key factors related to quality control, outline the major differences among currently available instrumentation, and understand the basic concepts related to computer functions associated with algorithms and filtered back projection which are key in the generation of SPECT images. Additionally, attendees should be able to list the major clinical applications of SPECT as they relate to each of the organ systems presented, and understand how SPECT generated data can be integrated into other non-radionuclide radiologic test results to aid in the diagnostic evaluation of the patient.

NOTES

SPECT IN CLINICAL PRACTICE

SPECT Imaging: How It Fits Clinically

Robert E. Henkin, M.D.

As SPECT applications continue to grow, the question is no longer whether or not SPECT has a place in clinical Nuclear Medicine but rather what its place is. As we see more and more applications being reported, we will have to try to evaluate those and decide which applications are most beneficial in the clinical situation for the relatively limited number of these devices available in most departments.

We will briefly describe a number of the major applications of current SPECT imaging.

CARDIAC

Without doubt, the major application for SPECT at the present time in most clinical laboratories, is the evaluation of thallium images. The advantages of the SPECT system over the previously available collimator system result primarily from the improved Z-axis resolution available to the SPECT user. Defects are generally not propagated heavily between the planes as occurs in the collimator systems.

Let us presume that SPECT imaging of the myocardium is indeed useful as has been suggested by Tamaki[1].

A number of laboratories have abandoned the routine planar clinical imaging in favor of SPECT only imaging. Our own laboratory has not done this since we have been able to accumulate a number of cases in which the SPECT image is the only correct data and others in which the planar image is the only correct data. We have, therefore, maintained a somewhat limited planar study while including the SPECT study as well.

Many systems are beginning to employ quantitative or semi-quantitative systems to evaluate the SPECT data. Several of these have been evaluated in our own laboratory. At this point, the level of sophistication of the quantitative system has not attained a dramatic enough or accurate enought status that permits the quantitative system to be relied on blindly. The creation of normal data pools for these studies is at best difficult. Normal data pools are not readily transferred from one institution to another. In addition, the protocols for acquisition for these automated analysis routines are so demanding that deviation from the protocol in any sense may invalidate the automated analysis.

Pyrophosphate imaging is also an area that has offered some potential yield in SPECT imaging although it is limited by the ability to transport the patients to the Nuclear Medicine Department.

Cardiac blood pool imaging, however, is beginning to show considerable promise. Several investigators have described techniques for doing single photon emission computed tomography of the cardiac blood pool using commercially available gamma cameras and computers. Some have been able to determine left ventricular volumes from this data. The correlation between cardiac catheterization and the radionuclide imaging has been quite good at approximately .85. Tomographic wall motion data has ageed well with that obtained at cardiac catheterization [2,3].

As yet, no commercial manufacturer has come forth with a package that does reliable volume determinations although several are in development.

Central Nervous System Imaging

This represents perhaps the most immediate application for SPECT in which there is essentially no competitive technology or planar imaging. Both the labeled amines and the technetium labeled brain perfusion agents, require SPECT imaging for adequate evaluation.

The major application to date, has been in studying cerebral vascular disease[4,5]. There is exciting evidence that the compounds may also be useful in localizing foci in epileptic patients[5]. The difficulty with the amine studies to date revolve primarly about the label with Iodine-123 and the availability of a suitable I-123 for labeling. More recently, there have been agents reported, and in use in Europe, that are technetium labeled. This may open a wider field of cerebral perfusion imaging to all hospitals with SPECT units.

Various analysis packages have been described for cerebral perfusion imaging. As yet, no standard agreement has been arrived at although these packages will be necessary as we get into more sophisticated stages of SPECT cerebral vascular imaging.

QNB, a compound designed to image muscarinic acetyl choline receptors is currently under evaluation at a limited number of sites, is a receptor pharmaceutical for brain imaging. This may prove the prototype of other compounds to come.

Liver Imaging

Data from our own laboratory as well as others, have indicated that liver imaging with SPECT is consideraly improved over standard planar liver imaging[6].

One of the advantages of the SPECT system with regard to liver imaging is the ability to quantitate the size of defects identified within the liver and spleen as well as to quantitate the absolute size of the liver and spleen themselves.

Changes as small as 10% in the volume of the liver spleen or liver lesion, may be accurately measured by a experimental system developed in our own laboratory.

As compared with transmission computed tomography and x-ray, there is no statistically significant difference between the lesion detection on either the SPECT study or on the TCT study.

Bone Imaging

A rapidly growing application for SPECT imaging is bone studies. There is clear evidence that SPECT has applications in detecting spinal malformations and subtle lesions in the spine, hips and knees that exceed the standard bone scan[7,8].

Gallium Imaging

Certainly, anything that can be done to improve the quality of gallium scans is worthwhile. Although gallium acquisition time is quite long in SPECT study, and several technical issues are not

completely resolved with regard to gallium imaging, we have noted a significant ability of the gallium scan to identify lesions that are not seen even on many tomographic studies from the Anger tomographic scanner. At the moment, we do not use SPECT as a primary tool for gallium imaging, but rather to investigate those areas that are either of special interest or equivocal on the survey study. It is, however, clearly evident that medistinal lesions, adrenal lesions and other interabdominal processes are better delineated on the SPECT study than on a standard tomographic study. Since the standard tomographic study is already acknowledged to be superior to the plain gamma camera study, this should represent a significant approvement over plain gamma camera studies.

Lung Imaging

Experimental studies have indicated that tomographic data can be obtained on ventilation and perfusion both using 81m krypton and 99m technetium aerosol [9]. Other studies using 99m technetium MAA and xenon-133 have reportedly reduced the number of false-positive or equivocal lung scans [10].

Summary

In summary, there are a number of studies that are available to the clinician at the present time, that he can justify employing SPECT as an adjunct to. It encompasses almost every area of Clinical Nuclear Medicine. Certainly, the areas that show the best promise at the moment for both quantitative and diagnostic improvement, remain the cardiac areas, bone scanning and liver. The central nervous system is in evolution and over the slightly longer term, should show tremendous clinical yield using SPECT techniques with some of the newer pharmaceuticals. However, even six or more years after the clinical introduction of SPECT technology, new applications are being reported relatively frequently. It is anticipated that there is no organ system that will not be amendable to SPECT study and the potential quantification that such a technique possess.

References

1. Tamaki N, Mukai T, Ishii Y, et al: Clinical evaluation of thallium-201 emission myocardial tomography using a rotating gamma camera: Comparison with 7 pinhole tomography. J Nucl Med 22:849, 1983.

2. Maublant J, Bailly P, Mestas D: Feasibility of gated single photon emission transaxial tomography of the cardiac blood pool. Radiology 146:837, 1983.

3. Underwood SR, Ell PJ, Jaritt PH, et al: ECG gated blood pool tomography in the determination of left ventricular volume, ejection fraction and wall motion. J Nucl Med 25:P87, 1984 (Abstr)

4. Holman BL, Hill TC, Lee RGL. et al: Brain scanning with radiolabeled amines, in Freeman LM, Weissman HS (eds): Nuclear Medicine Annual. New York, Raven Press, 1983.

5. Magistretti P, Uren R, Stromer D, et al: Emission tomographic scans of cerebral blood flow using iodine-123 iodoamphetamine in epilepsy, in Raynaud C (ed): Proceedings of the Third World Congress in Nuclear Medicine and Biology. Oxford, England, Pergamon Press, 1982, p 139.

6. Halama JR, Henkin RE: Single photon Emission Computed Tomography (SPECT) in Freeman and Johnson's Clinical Radionuclide Imaging, Third Edition Update, Grune & Stratton, P1529-1651, 1986.

7. Jacobsson H, Larsson SA, Vestershold L, et al: The Applications of single photon emission computed tomography to the diagnosis of ankylosing spondylitis of the spine. Br J Radiol 57:133, 1984.

8. Collier BD, Johnson RP, Carrera GF: Painful spondylolysis or spondylolisthesis studied by radiography and single photon emission computed tomography. Radiology 154:207, 1985.

9. Lavender JP, Al-Nahhas AM, Meyers MJ: Ventilation perfusion ratios of the normal supine lung ;using emission tomography. Br J Radiol 57:141, 1984.

10. O'Donnell JK, Golish JA, Gc RT, et al: Improved diagnostic accuracy of lung perfusion imaging using technetium-99m MAA SPECT. J Nucl Med 25:P67, 1984 (Abstr).

NOTES

SPECT IN CLINICAL PRACTICE

Review of Current Instrumentation

Robert T. Anger, M.S.

Tomographic imaging has been a part of nuclear medicine from the very beginning. Although not usually thought of as a tomographic imaging device, the rectilinear scanner technically produced longitudinal "tomograms" using a focused collimator to blur data from above and below the geometrically defined "depth of focus". Kuhl and Edwards (1963) "image separation radioisotope scanning", however, formally established the concept of single photon emission tomography in Nuclear Medicine. Development continued on dedicated multi-detector focused collimator transverse section systems, primarily for brain imaging, but the introduction and rapid development of the gamma camera in Nuclear Medicine and the CT scanner in Radiology kept these dedicated systems from having much impact in clinical nuclear medicine. The reconstruction algorithms developed for x-ray transmission tomography, however, provided a basis for further innovations in emission tomography. Software was developed for existing nuclear medicine computer systems that enabled short-axis tomograms of the heart to be obtained with standard gamma cameras using special collimation. Although these limited-angle approaches were not widely applied, the concept of single photon emission computed tomography (SPECT) was accepted as a reality and the central role of the gamma camera was established. After it was shown that transverse section imaging with full (360

degree) angular sampling was possible with the gamma camera, first by rotating the patient in front of the gamma camera detector and then by rotating the gamma camera detector around the patient, the way was paved for the introduction of the first commercially available gamma camera SPECT gantry in 1979. This presentation will review the developments in rotating gamma camera-based SPECT systems that have occurred since that date.

For descriptive purposes, rotating gamma camera SPECT system hardware consists of the gamma camera and gantry, the computer, and the camera/computer interface. The computer must, of course, have the software necessary to acquire, process and display the tomographic images. Complete systems can be purchased from a single manufacturer (a necessity in the case of those "digital gamma cameras" using an integrated gamma camera detector and digital computer), or a gamma camera/gantry from one manufacturer can be interfaced to a computer system from a different manufacturer. The latter approach offers more flexibility but may lead to camera/computer interface problems. A functional interface may still not support the full capabilities of either the gantry or the computer, and service problems not obviously attributable to either camera or computer can prove troublesome.

A state-of-the-art gamma camera is an essential component of the SPECT system. While the basic elements of the Anger

scintillation camera have not changed, there have been some improvements in design and performance characteristics particularly pertinent to SPECT:

Energy/linearity correction

Better scatter rejection

Autotuning

Higher count rate capability

Rectangular detectors

When comparing performance characteristics of gamma cameras, reference should be made to the NEMA "Standards for Performance Measurements of Scintillation Cameras" (1980,1986). The NEMA standards provide a uniform criterion for the measurement and reporting of scintillation camera performance parameters by which a manufacturer may specify his device, and, when doing so, reference the NEMA standards publication. By means of the NEMA standard, one can make meaningful intercomparisons of performance specifications for cameras from different manufacturers and on different models of cameras. Compliance with the NEMA standard is voluntary, but should be considered mandatory. The 1986 NEMA Standards do include some modified definitions and some additional performance parameters. The field-of-view definitions have been modified to accommodate non-circular detectors and the observed (rather than input) count rate at which a 20% count loss occurs will now be reported as both an intrinsic and a system (with scatter) parameter. Also,

the 1986 Standards contain three new parameters specifically addressing the performance of the gamma camera as part of a SPECT system:

Angular variation of flood field uniformity and sensitivity

Angular variation of spatial position

Reconstructed system spatial resolution

A guide to gamma camera/SPECT system comparisons can also be found in the ECRI/McGraw-Hill Nuclear Medicine Product Comparison System (1985). Although updating is required by reference to current performance specification sheets from individual manufacturers, comparisons are available for cameras, computers, and SPECT gantries. Reference is made where appropriate to applicable NEMA performance standards, but data is also provided with regard to mechanical and physical characteristics, such as size, weight, power requirements, heat loads, etc. A complete SPECT system requires a significant space commitment and required environmental characteristics are more rigorous than for the gamma camera alone.

A comparison of current model gamma camera performance characteristics would show relatively minor differences. SPECT system characteristics are much more variable due to differences in gantry design and the available computer hardware and software. Several different gantry designs are now available, some accommodating more than one detector.

The size, shape and shielding of the detectors are being modified to improve SPECT performance. New types of collimators are being considered. A minimum computer hardware configuration will provide minimum (and probably unsatisfactory) performance. The computer software must meet certain minimum performance characteristics and should offer at least the hope of continuing and easily incorporated updates. Patient contour tracking has been shown to improve system spatial resolution and contrast resolution, but this involves gantry and software requirements that may not be available for a particular SPECT system configuration. User-friendly software is an overworked term, but SPECT software should include apppropriate quality control procedures and offer the operator sufficient flexibility in filter design and selection, and in the display and manipulation of the tomographic images.

Gamma camera/SPECT systems are particularly attractive because the gamma camera is not necessarily dedicated to the performance of SPECT procedures. One must be aware, however, of the time constraints associated with SPECT procedures, which will depend in part on the sophistication of the hardware/software configuration. Each potential SPECT user must determine his minimum requirements for a SPECT system and then make sure that he has the opportunity to evaluate any commercially offered configuration to insure that the promises of the sales representative translate into actual system performance.

Recently published books by Croft (1986) and English and Brown (1986) provide thorough, straight-forward discussions of state-of-the-art SPECT technology. Croft in particular provides excellent chapters on instrumentation and computer hardware and software considerations.

REFERENCES

Kuhl, D.E. and Edwards, R.Q. Image separation radioisotope scanning. Radiology 80:653-666, 1963.

NEMA Standards Publication NU 1-1986, "Performance Measurements of Scintillation Cameras". NEMA Sales Office, 2101 L Street, N.W., Washington, D.C. 20037 (replaces NEMA Standards Publication NU 1-1980)

Nuclear Medicine Product Comparison System, Healthcare Information Services Division, McGraw-Hill Book Company, 1835 Underwood Blvd., Delran, New Jersey 08075, 1985

Croft, B.Y. Single-Photon Emission Computed Tomography. Year Book Medical Publishers, Inc., 1986

English, R.J. and Brown, S.E. Single Photon Emission Computed Tomography: A Primer. The Society of Nuclear Medicine, Dept 886J, 136 Madison Ave., New York, NY 10016, 1986

NOTES

SPECT IN CLINICAL PRACTICE

Understanding Algorithms

Bernard E. Oppenheim, M.D.

The reconstruction problem is to reconstruct a two-dimensional object from a set of one-dimensional projections of that object. Nowadays the problem is almost always solved by using the method of filtered backprojection, in which the projections are modified in some mysterious manner and then backprojected across the image plane, yielding a reasonable likeness of the object. The purpose of this paper is to provide an intuitive basis for understanding how and why this method works, based on the concept of the Fourier transform.

Fourier Transform. A projection can be represented by a one-dimensional function $f(x)$, representing the magnitude of the projection corresponding to each point x along the projection line. Any such function can be decomposed into a very large number of cosine waves, each wave having a specific wavelength, amplitude, and phase shift (shift along the projection line.) Each wave can be represented in one-dimensional frequency space (amplitude vs. frequency) by a single point, where the frequency is the reciprocal of the wavelength for that wave. (The amplitude is actually apportioned between a sine wave and a cosine wave of the same frequency, in order to represent the phase shift.) The plots for all the waves form the continuous function $F(\omega)$ in frequency space, where $F(\omega)$ is the amplitude of the cosine wave having wavelength $1/\omega$. We call $F(\omega)$ the Fourier transform of $f(x)$.

In a similar manner, an image can be represented by a two-dimensional function $f(x,y)$ which describes the brightness at each point (x,y) in the image. The function $f(x,y)$ can be decomposed in cosine plane waves, each having a specific wavelength, amplitude, phase shift, and direction in the plane. Each plane wave can be represented by a point in two-dimensional frequency space, and together these points form the continuous function $F(\omega,\theta)$ in two-dimensional frequency space, where $F(\omega,\theta)$ is the amplitude of the cosine plane wave in the direction θ, having wavelength $1/\omega$. We call $F(\omega,\theta)$ the two-dimensional Fourier transform of $f(x,y)$.

A smooth object is composed mostly of cosine waves with long wavelengths. These cosine waves have low frequencies, so that the frequency space representation of a smooth object (i.e., its Fourier transform) has non-zero values only in the region close to the origin. An object with prominent sharp structures will be composed of short and intermediate wavelength as well as long wavelength cosine waves. Since these waves will have high, intermediate, and low frequencies, the frequency space representation of the object will have non-zero values extending rather far from the origin.

Reconstruction by simple backprojection. Backprojection is the process of distributing a projection back across the plane to be reconstructed. It is employed by nearly all reconstruction methods. If this is the sole technique employed, then we have a crude form of reconstruction which is called simple backprojection. The image obtained by simple backprojection is badly blurred; its low frequency cosine wave components have large amplitudes, while its high frequency wave components have small amplitudes. The amplitude of the frequency space representation of the image falls rapidly with increasing distance from the origin. Now if one compares the frequency space representations of the original object and the image formed by simple backprojection, one finds that simple backprojection suppresses the amplitudes of the cosine waves in proportion to their frequencies (1). This provides the basis for the filtered backprojection method.

Reconstruction by filtered backprojection. This method can be implemented in various ways. The most straightforward conceptually is the two-dimensional frequency space approach. One first reconstructs an image by simple backprojection, then generates the Fourier transform of that image. Since the amplitude of the image at each frequency has been suppressed in proportion to the frequency value, one corrects for this effect by multiplying each of the amplitudes by its frequency $|\omega|$, boosting the high frequency components and suppressing the low ones. Here the term $|\omega|$ is the two-dimensional form of the well-known ramp filter. The resulting filtered image in frequency space is converted to a real space image via the inverse Fourier transform.

A more popular approach that is computationally more efficient involves filtering of the individual projections before backprojection. One performs a Fourier transform on each projection, multiplies the resulting frequency space function by the one-dimensional ramp $|\omega|$, then inverse Fourier transforms the result to obtain the filtered projection in real space. The filtered projections are then backprojected to obtain the reconstructed image.

One can completely avoid Fourier transforms by performing the filtering of the individual projections in real space by means of convolution. Space does not permit an explanation of this approach. Suffice it to say that while this was a very popular method in previous years, it is slower and less flexible than filtering in frequency space. Its chief advantage is a very compact algorithm (2).

In theory, filtered backprojection will produce perfect reconstructions if one is given an infinite number of continuous noise-free projections. In reality, one has a rather limited number of projections available, each consisting of discretely sampled values rather than being continuous, and each of these values being subject to random noise. The noise problem is handled by modifications of the filter which will not be addressed here, nor will other problems in reconstruction (attenuation, detector non-uniformity, scatter, varying resolution). We conclude with a discussion of the effect of sampling.

Sampling. Sampling implies representing a continuous object by measurements taken at fixed intervals. This does not necessarily result in a loss of information, provided that the object is sufficiently "smooth", with no significant frequency components beyond some cutoff frequency ω_c. Sampling a function in real space is equivalent to replicating the function in frequency space, a phenomenon known as "aliasing." The closer the samples, the further the separation of the frequency space replicates. If the sampling is performed at intervals no larger than $1/2\omega_c$ then the replicates will not overlap and all the information will be preserved.

The backprojection step of reconstruction requires continuous projections, so one must undo the sampling by means of interpolation, whereby the value between the sampling points is computed from the values of the sample points. The preferred method of interpolation is usually felt to be linear interpolation between the sampled values. Such interpolation eliminates the aliasing in frequency space at a cost of slight suppression of the higher frequencies. Nearest neighbor interpolation, in which one always uses the value of the closest sampling point, is computationally faster but can actually increase noise by enhancing some of the higher frequencies (3).

1. Budinger TF, Gullberg GT: Three-dimensional reconstruction in nuclear medicine emission imaging. IEEE Trans Nucl Sci NS-21:2, 1974.

2. Shepp LA, Logan BF: The Fourier reconstruction of a head section. IEEE Trans Nucl Sci NS-21:21, 1974.

3. Oppenheim BE, Appledorn CR: ART vs. convolution algorithms for ECT, in Deconinck F (ed): Information Processing in Medical Imaging. Boston, Martinus Nijhoff, 1984, pp 169-184.

NOTES

Looking at Things a Different Way: Filtering and Backprojection

Ernest V. Garcia, James R. Galt and H. Lee Hise

INTRODUCTION. Filtering is used extensively on Nuclear Medicine images to reduce statistical noise, enhance edges for edge detection, and in the reconstruction of tomographic images. Filtering can be performed in either the spatial domain or in frequency space (1). While many articles deal with operations in the spatial domain (1), the purpose of this presentation is to help develop intuition as to how to use frequency space without understanding complicated mathematical formulas. By exercising this intuition, one should be able to select filters for given applications, determine proper cutoff frequencies, and even design filters to meet the requirements of new applications.

FREQUENCY SPACE. Frequency domain methods of image enhancement deal with the spatial frequencies (cycles/centimeter or cycles/pixel) which make up the image. An image can be decomposed into a summation of different spatial frequencies. Spatial frequencies relate to the rapidity of change in intensity (counts) with distance. The high frequency components define edges, areas where there is a rapid change in intensity from bright to dark. Regions in an image where the changes are more gradual are primarily due to the lower frequency components. An example of such a region is the central area of the lobe of the liver from a high-count liver scan. While the concept of frequency space may appear difficult to grasp at first, when intuition is developed the principles can be more straightforward to apply than those used in the spatial domain (2).

In order to convert an image into its frequency components it is necessary to use an image transform, such as a Fourier transform, to transfer the image into frequency space. The Fourier transform

yields the frequencies that are present in the image and the amplitude of each frequency. An inverse Fourier transform transfers the image back into the spatial domain which is the conventional format for representing images. The method used by the computer (often with the aid of an array processor) to implement the Fourier transform is called a Fast Fourier transform (FFT). The FFT is a computer algorithm which has been optimized for speed.

FILTERING. Filtering in frequency space is accomplished by removing, or altering the magnitude of selected frequency components. Each specific frequency is multiplied by a factor assigned by the filter. If a particular frequency needs to be totally suppressed, the factor assigned to that frequency is set to zero. Filters that place emphasis on the low frequency components while reducing the high frequency components are called low-pass filters. If the opposite effect is desired, a high-pass filter is applied which reduces the low frequencies. A band-pass filter reduces both low and high frequencies allowing only a band of frequencies in between to remain.

The highest possible frequency which may be faithfully displayed (0.5 cycles/pixel) is called the Nyquist frequency. If the source image has more variations than the Nyquist frequency it will not be faithfully reproduced, and some information will be lost. This loss of information is called aliasing. A common example of aliasing is the way the spokes of wagon wheels in old westerns on television appear to rotate backwards while the wagon is going forwards. This occurs because the sampling rate of video (around 30 frames per second) is not fast enough to show a true representation of the wheel going forward. The positions of spokes of the wheels change more rapidly than the sampling rate. In the same way, if the image source has changes in intensity over a distance shorter than two pixels (at a higher frequency than the Nyquist frequency) the result will be an image that does not

accurately reflect the radioactive source distribution.

HANN FILTER. A common filter used in Nuclear Medicine image processing is the Hann filter. This low-pass filter is usually called a Hanning filter in the Nuclear Medicine field. The filter has a magnitude of one at the lowest frequencies and decreases to zero at a frequency known as the cutoff frequency. A Hann filter with a cutoff frequency of 0.5 cycles/pixel removes this and higher frequency components from the image. When this filter multiplies the same input image spectrum it can be seen that the 0.5 cycles/pixel frequency of the input image have been removed in both the filtered spectrum and image. The amplitude of the frequencies lower than .5 is reduced by the product of the filter value at those frequencies and objects related to these frequencies do not have as much contrast in the output image as in the input image.

POISSON NOISE. One of the primary reasons for applying low-pass (smoothing) filters is to reduce the high-frequency random noise associated with Poisson noise (statistical count fluctuations). The Hann filter appears to be better suited for studies where higher statistical accuracy is needed at the expense of a loss in spatial resolution.

BUTTERWORTH FILTER. Another low-pass filter is the Butterworth filter. Two parameters are needed to define the Butterworth filter, the cutoff frequency and the order of the filter. The order of the filter is related to how fast the filter is cut off, the higher the order the sharper the cutoff. The Butterworth filter may be applied using a sharper cutoff than the Hann filter, retaining contrast at higher frequencies while still eliminating the Poisson noise.

DEFINITION AMBIGUITIES. Before going on to clinical applications of filtering, a word of caution should be introduced about the terminology used by the Nuclear Medicine industry in describing

filters. While some manufacturers define the cutoff frequency at the point where a filter value drops to zero, others define the cutoff frequency as the point where the filter magnitude drops below a given value. The meaning of the term cutoff frequency may also differ for different kinds of filters (even by the same manufacturer). It is also important to define the units being used when speaking of frequencies. Frequencies may be defined as cycles/pixel, cycles/centimeter, or in any number of other units. Unless it is clear which units are being used, and how the cutoff frequency is defined, inappropriate values may be used to define filters, resulting in improper filtering.

TOMOGRAPHY. The basic process for reconstructing tomographic images has been presented elsewhere (3). Tomographic projections are nothing more than a series of planar images taken at different angles around the patient. These images are then backprojected into transaxial images. The transaxial images can then be re-oriented to produce sagittal, coronal or oblique angle images. As with planar images, tomographic projection data includes a certain amount of noise. This noise, however, is amplified in the backprojection technique and causes the resultant transaxial information to appear different from the radioactive distribution being studied (1).

More specifically, the goal of tomographic reconstruction is to provide a blur-corrected transaxial tomogram from processed planar projections. The solution to this problem in frequency space involves the application of a Ramp filter to the frequency components of each projection. Once filtered, each projection is transformed back into the conventional spatial domain and then back-projected to form the blur-corrected transaxial tomograms.

The Ramp filter is a high-pass filter. Previously it was explained that high-pass filters enchance the edges of the

radioactive distribution in the image. Intuitively, the reconstruction process known as filtered backprojection may be thought of as first extracting the edges of a three dimensional radioactive source from different angles and second backprojecting the edges from the different angles to generate the count distribution in a transaxial tomogram. The Ramp filter, being a high pass filter that linearly enhances higher frequencies, yields the highest resolution possible in a reconstruction but also propagates the high frequency noise associated with low count statistics. This propagation of noise often results in clinically uninterpretable images.

Modification to the Ramp filter must be made to compensate for the undesirable noise. This is done by combining the Ramp characteristics with those of a low pass filter or window. Hanning and Butterworth filters are two commonly used windows that can be multiplied by a Ramp filter to yield different degrees of trade-off between reduction of statistical noise versus degradation of spatial and contrast resolution.

Noise can be removed from the final tomograms either by applying the filters to the planar projections prior to backprojection (filtered backprojection) or afterwards by filtering the transaxial slices (post-processing filtering). Whether to filter before or after back projection, remains debatable. It may be argued that filtering prior to back projection is more desirable for two reasons. First it reduces the propagation of noise at an earlier stage in the image formation process and second it promotes the implementation of a filter symmetric in three-dimensions (same resolution in the X, Y and Z directions). Proponents of post-processing would argue that the same results could be obtained by the careful selection of filters applied to the transaxial tomograms.

One of the more interesting properties of frequency filtering

is that once a frequency has been removed from an image by a filter, further processing will not bring that frequency back to the image.

References

1. Garcia EV: Digital Processing in Nuclear Medicine Imaging. JNMT Vol. 14: Number 1: March 1986

2. Baxes GA: Digital Imaging Processing. Prentice Hall, New Jersey, 1984

3. Eisner RL: Principles of Instrumentation in SPECT. JNMT Vol. 13: Number 1: March 1985

NOTES

SPECT IN CLINICAL PRACTICE

Effects of Attenuation in SPECT

Stephen C. Moore, Ph.D.

The general goal of any SPECT imaging procedure is to obtain cross sectional image(s) of the intensity distribution of a given radionuclide in a given organ. These images are usually reconstructed from a complete set of projection images, each acquired at a different angle, by using a standard reconstruction algorithm, such as filtered backprojection. It is straightforward to show that an "exact" analytic reconstruction can be obtained (in the limit of infinitely fine sampling and an infinite number of counts) only if the number of counts measured for each projection ray is directly proportional to the line integral of the activity distribution along the ray.

Unfortunately, there are several physical effects which violate this requirement for an exact, analytic reconstruction. The effects to be considered in this presentation are (1) attenuation of emitted photons, and (2) scattered photons which are detected. After emission, a gamma photon can either escape the body unattenuated, or it can be attenuated by being scattered (one or more times) or by being absorbed photoelectrically. The direct, unattenuated photons and the scattered photons are both candidates for detection. To be considered detected, they must pass through the collimator, presumably along a "legitimate" projection ray, and then deposit an amount of energy in the detector which falls within the energy "window" selected by the operator.

Photons which scatter in the patient and are then detected violate the requirement (defined above) for an exact analytic recontruction because they are not detected along the projection ray which traverses their original point of emanation; that is, they "appear" to come from a different source point in the body. Photons which are attenuated (i.e., scattered and not detected, or else photoelectrically absorbed in the body) cause problems because the probability of absorption depends on the depth of the source within the body. This leads to an ambiguity in the measurement of the projections, which is illustrated in Figure 1. It is easy to see that we could obtain the same measurement along the projection ray, P, by imaging a strong source, A, attenuated by length, d_A, or by imaging a weaker source, B, attenuated by the shorter distance, d_B. The measurement process couples the desired activity distribution to the distribution of attenuating material in a complex manner.

FIG. 1

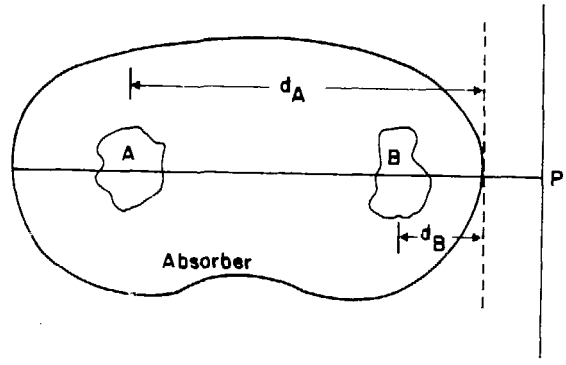

Effects of Attenuation

For a narrow-beam, monoenergetic source, the total percentage of photons transmitted through a given thickness of water absorber is shown in Fig. 2 for 80 keV and 511 keV. The transmission is, of course, an exponential function of absorber thickness. The probability of transmission of 140 keV photons (which falls between the two curves) through 10 cm of water is only ~22%. Although the attenuation decreases for higher energy photons, it may be seen that even 511 keV photons have less than a 40% chance of traversing 10 cm of water without being scattered or absorbed. Thus attenuation is also a problem for PET scanning; however, it may be corrected for more easily than in SPECT because of the simultaneous detection of two back-to-back photons.

FIG. 2

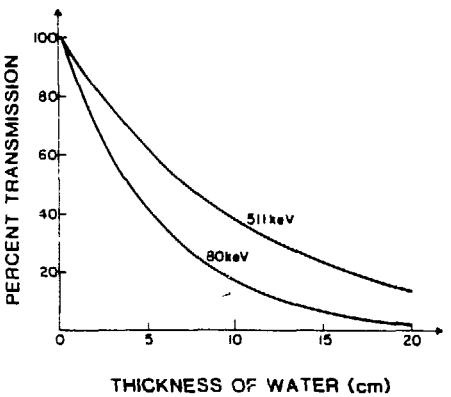

Shown in Fig. 3 is a SPECT image of a 20-cm-diameter cylindrical phantom with a uniform activity concentration of Tc-99m, reconstructed by filtered backprojection with no attempt to correct for attenuation.

FIG. 3

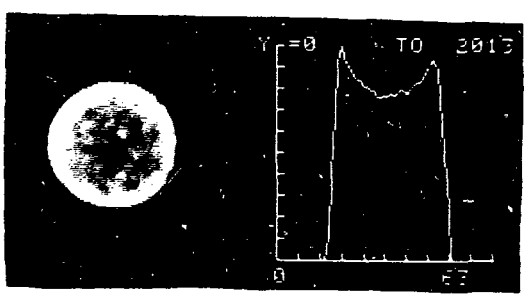

Approximate Attenuation Compensation Methods

Most commercially available rotating camera systems provide an approximate, or "first-order" attenuation compensation procedure as part of their image reconstruction software. Two general classes of such methods are (1) post-correction, and (2) pre-correction algorithms. We will describe one example of each, although other simple methods have been proposed.

The post-correction algorithms try to correct for the effects of attenuation by correcting an image AFTER reconstruction using filtered back-correction. Chang (1978) proposed that the multiplicative correction factor applied to a given pixel in the image should be the inverse of the average attenuation along lines from that pixel to the patient boundary in all directions. Mathematically,

$$\text{Corr.}(x,y) = 1 \Big/ \left[\frac{1}{M} \sum_{i=1}^{M} \exp\left(-\mu \ell(x,y,\theta_i)\right) \right]$$

where μ is the linear attenuation coefficient for the appropriate gamma ray energy in water, M is the number of projections, and $\ell(x,y,\theta_i)$ is the distance from the point (x,y) to the boundary of the attenuating material along the relevant projection ray at angle θ_i. If the true distribution of attenuating material is known, this correction factor can be modified by numerically integrating the attenuation distribution along the lines $\ell(x,y,\theta_i)$. Using this method, Jaszczak et al. (1981) reported reasonably accurate (within 10%) reconstructions of spherical sources in a uniform cylindrical background of a different activity concentration. For more unusual source and attenuation distributions, however, this method is not expected to work as well since it cannot resolve the fundamental measurement ambiguity demonstrated in Fig. 1.

FIG. 4

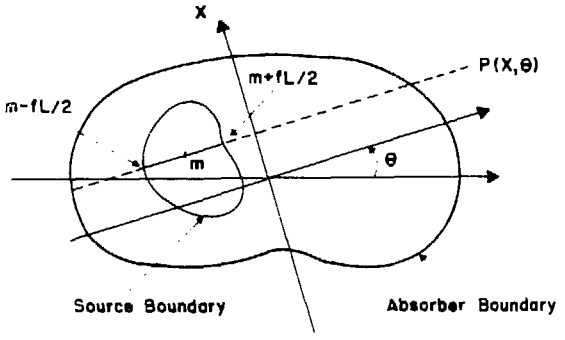

The most commonly used pre-correction technique, in which the projection data are corrected for attenuation BEFORE reconstruction, is known as the Sorenson (1974), or "hyperbolic sine" correction. This method requires that the projections be measured over 360 degrees because the correction is applied to the geometric mean (the square root of the product) of opposing projection rays. Although this method is usually implemented with the assumption that the source distribution fills the region of attenuating material, the correction can be implemented more accurately if the approximate location, size, and shape of a small source inside a larger attenuating medium is known. Assume that we have a region of uniform activity distribution within a larger absorbing medium of constant attenuation, μ. (See Fig. 4.)

If a measured projection ray traverses a distance L of absorber, along which the fractional length, fL, has a constant source strength, C, then the attenuated projection data, $p(x,\theta)$, is given by:

$$p = p(x,\theta) = \int_{m-\frac{fL}{2}}^{m+\frac{fL}{2}} C\, e^{-\mu(L-l)}\, dl$$

where m is the mean source depth within the absorber. Its conjugate, or opposing, projection ray will be:

$$p_{conj.} = p(-x, \theta+\pi) = \int_{m-\frac{fL}{2}}^{m+\frac{fL}{2}} C\, e^{-\mu l}\, dl$$

Integrating these two equations and calculating the geometric mean gives:

$$\left[p \cdot p_{conj.}\right]^{1/2} = \frac{2C}{\mu}\, e^{-\mu L/2} \sinh\left(\frac{\mu f L}{2}\right)$$

Since we would have measured $p(x,\theta) = CfL$, in the absence of attenuation ($\mu = 0$), it is easy to see that a corrected projection, p', can be obtained by calculating:

$$p'(x,\theta) = \left[p \cdot p_{conj}\right]^{1/2} \left(\frac{\mu f L}{2}\right) \frac{e^{\mu L/2}}{\sinh(\mu f L/2)}$$

The length of each projection ray through the absorber, L, can be calculated from an assumed or measured body contour. The attenuation, μ, can be assumed equal to that of water, for example. The fractional length of the source distribution, f, can be estimated from an initial reconstruction without an attenuation correction. However, as already described, most implementations of the Sorenson correction simply assume that f = 1, which corresponds to the case of a uniform source completely filling the region of attenuation.

More exact (and more elaborate) attenuation compensation procedures have been investigated and described by many authors; however they are beyond the scope of this presentation. A description of several different algorithms -- both analytic and iterative -- may be found in a review by Moore (1982).

FIG. 5

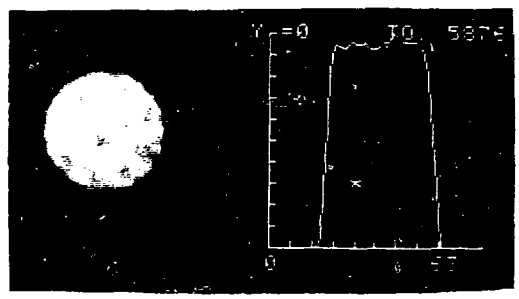

The Need for Scatter Compensation

Shown in Fig. 5 is a reconstructed image of the same source shown in Fig. 3, but after attenuation compensation with the Sorenson pre-correction method. This phantom contained a uniform concentration of Tc-99m in water. For this case, the narrow-beam linear attenuation coefficient is 0.15 cm^{-1}; however, the value of the linear attenuation coefficient, μ, used in the correction program to produce the image in Fig. 5 was less than 0.15 cm^{-1}. The discrepancy can be explained by the fact that our projection measurements do not satisfy the requirement of "narrow-beam" geometry, i.e. the projections contain scattered photons. While it may be possible to find an "effective" μ which makes a uniform source appear "flat", this technique does not really eliminate scattered photons from the projection data. This means that there will always be a scatter background -- usually non-uniform -- in our reconstructed images. This background is most evident in images which contain "cold" regions, e.g. Fig. 6a.

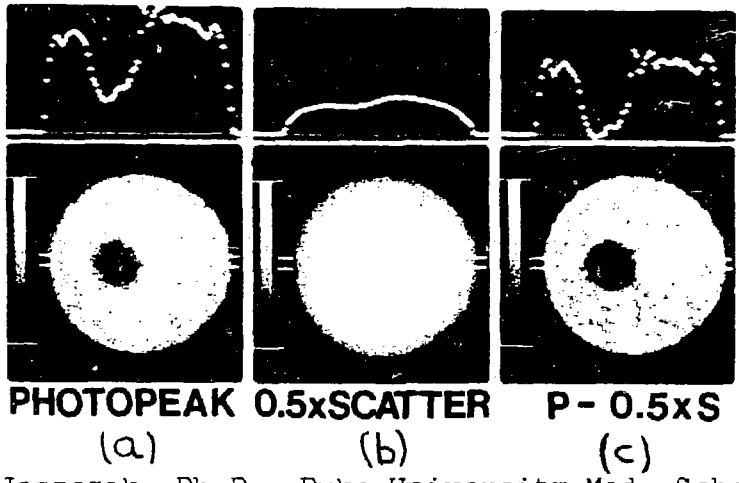

FIG. 6 SPECT images and histograms of photon-deficient sphere (6 cm diam) placed within water-filled cylinder (22 cm diam) containing uniform distribution of Tc-99m.

(Courtesy of Ronald J. Jaszczak, Ph.D., Duke University Med. School)

For Tc-99m in water, typically 40% of all detected photons are scattered at least once before being detected in a 20% energy window (126-154 keV). Single- and multiple-order scattered photon energy and spatial distributions have been described using Monte Carlo simulation techniques by Floyd et al. (1984).

Shown in Figure 7 are the contributions to the energy spectrum of a line source of Tc-99m in a water-filled cylindrical phantom from various orders of scatter. It can be appreciated from this figure that many of the photons detected in the energy window have scattered through large angles and carry little information about the original source position. These photons produce long "tails" on the reconstructed system point spread function.

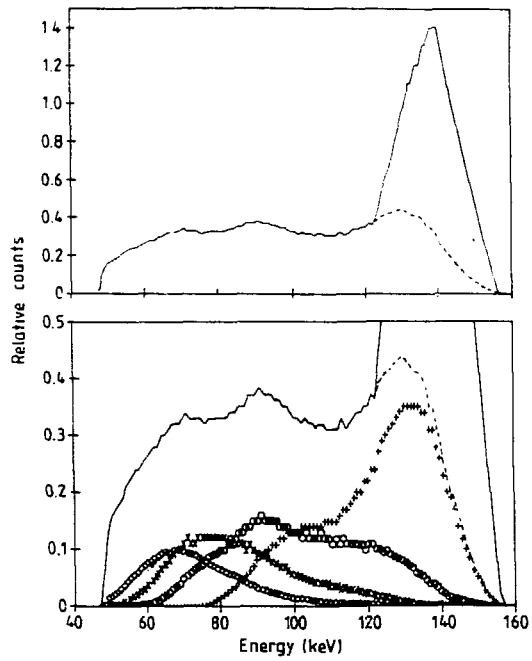

Figure 7 Energy spectra with the source on-axis for the SPECT acquisition showing the total spectrum as well as the separated scattered spectra. Key: Solid line, all counts; broken line, all scatter. +, 1st order; ○, 2nd order; ×, 3rd order; ◇, 4th order.

(Courtesy of Carey E. Floyd, Jr., Ph.D., Duke University Med. School)

Although many elaborate methods of scatter compensation have been proposed (for a nice review, see Jaszczak (1985)), two simple approaches are (1) subtraction of a "scatter image" from a photopeak+scatter image (Jaszczak, 1984), and (2) deconvolution of images for the tails on the point spread function (Axelsson et al (1984) and Floyd et al (1985)). Figure 6c demonstrates the improvement possible when the scatter image subtraction method is used. This method, of course, requires the simultaneous acquisition of projection data in a lower energy scatter window.

REFERENCES

Axelsson B, Msaki P, Israelsson A (1984). Subtraction of Compton-scattered photons in single photon computerized tomography. J. Nucl. Med. 25: 490-494.

Chang LT (1978). A method for attenuation correction in radionuclide computed tomography. IEEE Trans. Nucl. Sci. NS-25: 638-43.

Floyd CE, Jaszczak RJ, Harris CC, Coleman RE (1984). Energy and spatial distribution of multiple order Compton scatter in SPECT: a Monte Carlo investigation. Phys. Med. Biol. 29: 1217-1230.

Floyd CE, Jaszczak RJ, Greer KL, Coleman RE (1985). Deconvolution of Compton scatter in SPECT. J. Nucl. Med. 26: 403-408.

Jaszczak RJ, Coleman RE, Whitehead FR (1981). Physical factors affecting quantitative measurements using camera-based single photon emission computed tomography (SPECT). IEEE Trans. Nucl. Sci. NS-28: 69-80.

Jaszczak RJ, Greer KL, Floyd CE, Harris CC, Coleman RE (1984). Improved SPECT quantitation using compensation for scattered photons. J. Nucl. Med. 25: 893-900.

Jaszczak RJ, Floyd CE, Coleman RE (1985). Scatter compensation techniques for SPECT. IEEE Trans. Nucl. Sci. NS-32: 786-793.

Moore SC. (1982). Attenuation compensation in single photon emission tomography. In: Ell PJ and Holman BL, eds. Emission Computed Tomography. Oxford: Oxford University Press; 339-360.

Sorenson JA (1974). Methods for quantitative measurement of radioactivity in vivo by whole-body couting. In: Instrumentation in Nuclear Medicine, Vol. 2 (eds. G.J. Hine and J.A. Sorenson) New York: Academic Press; 311-348.

NOTES

SPECT IN CLINICAL PRACTICE

Uniformity Requirements in SPECT

Gerd Muehllehner, Ph.D.

NOTES

SPECT IN CLINICAL PRACTICE

Clinicians Guide to Technical Artifacts

John W. Keyes, M.D.

There are a large number of artefacts which occur in SPECT images, some of which are serious enough to render the images unreliable for diagnostic purposes and most of which (but not all) are readily recognizable to the trained eye.

Most SPECT artefacts arise as a consequence of poor or incomplete quality control. Unlike conventional nuclear medicine imaging, which is relatively forgiving of minor deviations of instrument performance from optimism, SPECT can magnify seemingly trivial problems into glaring defects in the final images. The need for a high degree of field-flood uniformity has been stressed elsewhere. The characteristic bull's eye artefact produced by uncorrected camera nonuniformities should be easily recognizable to all clinicians and technologists performing SPECT.

Other elements of quality control including proper calibration of the center-of-rotation and proper pixel size calibration are also of extreme importance, especially as minor errors in these parameters can seriously degrade image quality without producing a recognizable discrete pattern. Improper alignment of the camera head parallel to the axis of rotation likewise can produce serious errors in the reconstructed images and yet be unrecognizable to the exploring eye.

Several types of artefacts relate to patient positioning within the camera gantry. The most common of these is the arm-shadow artefact produced by leaving the patients' arms at the side of the body during liver/spleen SPECT. We have demonstrated this to be a serious source of interpretive error. A characteristic star-burst artefact can be produced from residual tracer at the injection site if this lies at the periphery of the image field. A final problem related to data acquisition is noisy images related to insufficient counts in the projection data.

A final source of artefacts is improper reconstruction of the data into tomograms. Problems include the wrong choice of filters (either too smooth or too sharp), lack of attenuation correction and wrong choice of slice thickness if reformatting the data into nontransaxial planes.

This presentation will show examples of all of these artefacts with emphasis on recognition of the artefact in the final image and correction of the problem.

References

Harkness BA, Rogers WL, Clinthorne NH, et al: SPECT: Quality control procedures and artifact identification. J Nucl Med Tech 11:55-60, 1983.

Rogers WL, CLinthorne NH, Harkness BA, et al: Field flood uniformity for emission computed tomography with an Anger camera. J Nucl Med 23:162-168, 1982.

Greer KL, Coleman RE, Jaszczak RJ: SPECT: A practical guide for users. J Nucl Med Tech 11:61-65, 1983.

Gottschalk SC, Salem D, Lun CB, et al: SPECT resolution and uniformity improvements by noncircular orbit. J Nucl Med 24:822-828, 1983.

NOTES

SPECT IN CLINICAL PRACTICE

Practical Aspects of Quality Assurance

Robert E. Henkin, M.D.

The great philosopher, Pogo, is reported to have said that he had met the enemy and they are us. Certainly, with regard to SPECT, this is the case.

Many individuals operating clinical SPECT units have not taken the trouble to develop the appropriate quality assurance protocols to verify the correct operation, positioning and reconstruction of data. The result in many institutions is mass confusion. Artifacts run rampant and faith is lost in the system due to misdiagnosis.

Without the availability of a quality control routine that is both adhered to and evaluated, the generation of clinically valid SPECT data is not possible. Below I will list some of the considerations that need to be dealt with in developing such a system.

Detector Gantry Alignment

The mechanical misalignment of components in the Gantry system may be expected to occur on a relatively routine basis due the heavy weight of the object being rotated. This misalignment can often be identified visually by looking at the following criteria:

1. Is the imaging table centered on the axis of rotation of the camera?

2. Are the X and Y axis aligned perpendicular and parallel respectively to the axis of rotation?

3. Does the plane of detector remain parallel to the axis of rotation as the detector rotates?

Computer Center of Rotation

The assumption that the center of rotation of a gamma camera using a 64 x 64 matrix with SPECT acquisition is 32, is at first incorrect and secondly dangerous with regard to reconstruction artifacts. Errors of one pixel in the center of rotation produce significant artifacts in the data. Ideally, this parameter should be known to the nearest tenth of a pixel.

There are various methos of obtaining the center of correction, no one of which is better than the other. However, it is important to both know where the center of rotation is and to know where it was previously. Significant changes in the center of rotation indicate a malfunction in the computer or the gamma camera.

Uniformity

The majority of artifacts that we identify on SPECT studies result from uniformity problems. The uniformity correction commonly applied to SPECT studies results from a thirty million count flood generated for a specific collimator. Since the majority of the correction is correcting for collimator errors, this flood may not be utilized with other collimators. Each collimator requires its own flood.

The thirty million count flood should be inspected for uniformity. It is necessary that the corrected data have a uniformity of plus or minus one percent. However, the input data will never be quite that good. The use of uniform sheet sources is the most convenient and in many respects the only viable means of obtaining flood correction data. Liquid filled sources have mechanical problems associated with them as well as potential mixing and contamination problems. In obtaining a solid sheet source, specifications for the source should be plus or minus one percent across the field of view, otherwise, it will never be possible to obtain the necessary one percent uniformity correction.

Uniformity correction is applied to virtually all SPECT studies. There are some cases in which this application may not be necessary. Specifically, thallium SPECT due to the low count nature of the study may not require uniformity correction.

It is also necessary in these systems to determine pixel calibration. The size of each pixel is used during the attenuation correction process in most systems. Additionally, if the X and Y diameters of pixels are not the same, the analog to digital converters in the computers are undoubtedly miscalibrated.

Last, but not least, collimators themselves should be evaluated. Obvious collimator artifacts are going to result in SPECT artifacts. However, more subtle manufacturing errors in a collimator such as having the septa not precisely parallel, will result in SPECT errors as well. The easiest way to evaluate such collimators is both with a high count flood and to compare the center of rotation of the collimator in question to center of rotation obtained with other collimators that are known to meet acceptance criteria.

Errors in reconstruction of clinical data are often masked by noise. Therefore, it is recommended that one or more phantoms be obtained and routinely evaluated on the system. Both hot and cold spot resolution, the effects of volume averaging in the area, of a checkerboard pattern, and other important SPECT parameters may be judged from these known configuration phantoms. These errors in the operation of the system will be detected more readily than in the clinical studies. They will also be detected before they can affect the clinical data.

The performance of SPECT without adequate quality assurance leads to inaccurate patient diagnosis as well as loss in confidence of the ability of the SPECT system to perform. Strong quality assurance protocols must be established prior to the clinical use of all SPECT systems. That protocol must be adhered to on a continuing basis.

For further discussions, the reader is referred to the Du Pont Guide to Instrument Quality Control for Nuclear Medicine.

NOTES

SPECT IN CLINICAL PRACTICE

Technical Aspects

Summation

Bernard E. Oppenheim, M.D.

NOTES

SPECT IN CLINICAL PRACTICE

Patient Set-Up for SPECT

Barbara Y. Croft, Ph.D.

The marriage of an familiar instrument of nuclear medicine, the Anger camera, with the much more forbidding-looking gantry of the x-ray CT scanner to form the SPECT instrument is making us look at positioning and patient examination parameters in a new light. In this discussion, I am assuming a SPECT system in good working order which receives regular and thoughtful quality control.

The dilemma of nuclear medical imaging is to collect the greatest number of counts with the best resolution in a fashion consistent with low radiation dose and patient comfort. Let us examine each of these requirements and its effect on the examination.

The collection of the counts available in the most efficient way involves the selection of camera parameters, such as the energy window and its width and the collimator, and of computer parameters, such as matrix size, and of SPECT motion parameters, such as the number of angles, and the amount of time to spend at each angle. During reconstruction, choices of slice thickness, filter, smoothing parameters, attenuation correction, etc, will affect the quality of the image, or fail to make the most of the information available.

The best resolution of the Anger camera is at the face of the collimator. This fact must not be lost sight of in the excitement of seeing a camera rotate around a patient. The methods for keeping a rotating camera close to the patient, who is far more elliptical than round, are several. It is my opinion that the best of these involve an elliptical motion, combining vertical and horizontal motions, so that the center of the camera's rotation is always in the center of the camera's field of view. This may be accomplished by the camera head alone, by the imaging table alone, or by a combination of camera and table motions. The practical effect of this elliptical motion is to allow the organ being imaged to be in the field of view at all angles. This is necessary if all of the organ is to appear on the final transaxial images.

Geometry for SPECT imaging requires that the camera collimator holes be perpendicular to the axis of rotation for the whole examination. For straight-hole collimators, this means that the collimator face is parallel to the the axis of rotation. If an angled collimator is being used, the angle should still be such that the collimator holes are perpendicular to the axis. The engineering of the instrument should make assuring such geometry a simple matter.

Nothing that interferes with this closeness or that inserts an extra layer of scattering material should be tolerated. The

patient's arms must not be at the sides during torso imaging. Elaborate restraint devices must not intrude between the patient and the camera. Clearly the same precautions about watches, belt buckles, wigs, etc, must be observed for SPECT as for planar camera imaging. Pendulous breasts should be considered; especially beware of their shifting position during the examination.

The requirement for low radiation dose makes us examine once again the relationship between counts, resolution, activity injected, and radiation dose. If the activity injected is doubled, keeping everything else constant, the counts will double and the uncertainties will be multiplied by 0.707. The activities that are used for SPECT are often at the upper limit of those allowed in the package insert, but each practitioner must ascertain that this is the best choice for each patient.

The requirement for patient comfort is evident in the design of the imaging table. (I think there is no longer a movement to keep the patients on their feet, standing on a turntable rotating in front of a stationary camera.) Because the examination will last 20 to 40 minutes, during which time the patient must not move, various aids to comfort should be experimented with: raised knees if the legs don't interfere with the gantry motion, a towel under the small of the back, something for holding the arms out of the field of view for torso imaging, prone vs. supine positioning, sheepskin padding for unpadded tables. If it is possible for the patient to be either head in or feet in, the torso may be imaged with the feet in and the arms supported by a trapeze suspended from the ceiling over the patient's head. Such maneuvers may also lessen the chance of wrapping IV lines, etc, around the moving gantry.

The patient should be gently and firmly strapped to the imaging table and warned that even motion of parts of the body not being imaged could cause the organs being imaged to move.

Because patients will still move and because we would like to have some measure of what their motion was, I suggest the placement of two or more sources on the patient during the examination. These should be of such activity that they do not dominate the images. During cine replay of the examination the sources can be examinated for their stability. The sources can also be used in the creation of a sinogram, which in its turn may actually be used to reposition the individual images for more accurate reconstruction.

Head SPECT presents special problems for the instrument as well as the technologist. The instrument should be designed so that the thickness of shielding and extra PM tubes (I call it the "rind") around the active surface of the camera face is not too thick, making possible the imaging of the head and neck with the camera close to the skin surface at all angles. Systems with a 180-degree angled collimator present a variation on this theme, but do not give the best resolution at the base of the brain and

in the bones of the neck.

Technologist's compassion for the patient may save what might be a bad examination. If the technologist will talk to the patient, hold a hand, and engage the patient's attention, the time will pass faster for both of them and there will be less patient motion.

REFERENCES:

Croft BY. Single-Photon Emission Computed Tomography. Chicago: Year Book Medical Publishers, 1985. Chapters 5, 7.

Greer, KL, Coleman RE, Jaszczak RJ. SPECT: a practical guide for users. J Nucl Med Tech 11:61-65, 1983.

Harkness BA, Rogers WL, Clinthorne NH, Keyes JW Jr. SPECT: quality control procedures and artifact identification. J Nucl Med Tech 11: 55-60, 1983.

NOTES

SPECT IN CLINICAL PRACTICE

Current Advances in Hepatic SPECT Imaging

Ronald L. Van Heertum, M.D.

HEPATIC SPECT IMAGING

In the abdomen, SPECT imaging has primarily been used in the evaluation of disorders of the liver and spleen. Although Technetium-99m sulfur colloid (SC) remains the most popular radiopharmaceutical for this examination, similar results can be obtained with other colloids including technetium microaggregated albumin.[1]

Imaging commences approximately 20 minutes post-injection of 4-5 mCi of Tc-99m colloid. The patient is positioned supine on the imaging couch with the head towards the gantry. The patient's arms are placed over the chest or behind the head in a position clear of the liver and spleen. The liver and spleen are centered so as to remain within the detector field of view throughout the entire acquisition and the patient is instructed to breathe quietly. The actual acquisition technique consists of acquiring 64-128 views at 10-20 seconds per view over a 360 degree circular rotation orbit. The images are either uniformity corrected "on the fly" or at the completion of the procedure. At the end of the study the quality of the acquired data is assessed using both closed-loop cine and sinogram displays. The latter is generated from a horizontal ROI profile taken from all the projection images at the level of the superior aspect of the liver. The cine display is also utilized to gain additional diagnostic information, particularly as regards localization of disease.

After uniformity correction, the acquired data undergoes attenuation correction. The projection images are then either preprocessed using two-dimensional spatial filters or post-processed after reconstruction using three-dimensional filters. The actual reconstruction process consists of filtered back projection with a ramp filter (cut off frequency 10 cycles/pixel).

The images are routinely reconstructed, displayed and interpreted in contiguous 6-12 mm width sections of the transaxial, coronal and sagittal planes. Oblique angle reconstructions are only used in select cases for evaluation of questionable vascular or ductal structures.[2]

The transaxial images are displayed in classic transmission CAT format. The sections begin inferiorly at the margin of the right lobe, porta hepatis, left lobe and spleen. The porta hepatis is the most difficult area to interpret as there is a wide spectrum of normal variations.

The coronal sections are displayed in the same orientation as an anterior planar image. The sections begin anteriorly in the left lobe with contiguous sections extending into porta hepatis, right lobe and the entire spleen. In addition to the porta hepatis, other areas with potential anatomic variation include the left lobe, gallbladder fossa, right renal fossa, hepatic vein insertion site and right lobe.

The sagittal sections are displayed in the same format as a right lateral planar view of the liver. The sections begin on the patient's left side with consecutive sections through the spleen, the left hepatic lobe, the porta hepatis and finally the right lobe. Oblique angle reconstructions are only performed in difficult to diagnose cases as an adjunctive means of identifying ductal and/or vascular structures. On occasion, it is helpful to inject additional radiopharmaceuticals such as a hepatobiliary, blood pool, or renal agent on a concurrent basis in order to obtain further diagnostic information.

Liver-spleen SPECT imaging has been reported to be most useful in the evaluation of focal liver disease. A number of separate studies have demonstrated that the SPECT technique is superior to planar liver-spleen imaging with accuracy rates in

the range of 90-94%.[3,4] The greater accuracy of the procedure appears primarily to be related to improved image contrast and better spatial resolution at increasing distances from the surface of the detector.[5] The SPECT technique appears to be most accurate when displayed and interpreted in at least three planes. The three plane approach is particularly important in the evaluation of presence and extent of disease, as well as in the differentiation of intra versus extra-hepatic disease.

Hepatic SPECT imaging, also compares quite well with transmission CAT (TCT) scanning.[6,7] Both modalities appear to have specific strengths and weaknesses. The SPECT technique is superior to TCT in the evaluation of diffuse liver disease.[8] SPECT imaging is also quite useful for the assessment of both superficial defects and deeper defects throughout the liver. Conversely, the porta hepatis is the area that is most difficult to evaluate with this technique. Transmission CAT scanning, on the other hand, can be very useful for the assessment of the porta hepatis and is also helpful for the evaluation of focal disease in most of both lobes of the liver.

Our current institutional approach is to recommend the liver-spleen SPECT examination as the first procedure for evaluation of known or suspected focal and diffuse space-occupying liver disease. Those SPECT cases that are equivocal or in need of additional diagnostic information are then referred for a dynamic CAT scan. Negative studies on the other hand, do not as a general rule undergo any further examination.

Nuclear Medicine laboratories with limited SPECT imaging capability and a heavy case load of conventional planar scans need to carefully triage their cases. One useful approach is to perform an anterior planar image of the liver in all

cases suspected of space-occupying liver disease. If the anterior planar image is positive, the planar examination should be continued on a planar imaging device. Conversly, a SPECT examination without additional planar images is performed when the anterior planar image is negative. Such an approach should result in maximum utilization of all available imaging devices.

The current indications for performing the SPECT examination in the case of suspected or known space-occupying liver disease include: 1) detection of disease; 2) definition of extent and location of disease, and 3) follow-up. In addition, in cases of primary liver tumors, the examination is also useful in defining resectability of the lesion.

HEPATIC BLOOD POOL SPECT IMAGING

Hepatic blood pool SPECT imaging is a more recent development than the above described technique. This approach evolved as a means of further defining the anatomy of the porta hepatis.[9] In essence, the technique consists of the intravenous injection of 20 mCi of Tc-99m pertechnetate after pre-loading with stannous pyrophosphate for in-vivo labeling of red blood cells. The imaging procedure commences 5-10 minutes post-injection. During the acquisition phase, 64-128 images, at 10-20 seconds per image, are collected over a 360 degree rotation orbit. The resultant images are routinely displayed in the coronal, sagittal and transaxial planes. Oblique coronal reconstruction in a plane parallel to the spleno-portal axis is frequently used for evaluation of the spleno-portal axis. The indications for hepatic blood pool SPECT imaging include: 1) evaluation of the vascularity of various types of liver tumors; 2) assessment of major vessel patency, and 3) diagnosis of hepatic hemangioma.

In the evaluation of primary and secondary liver tumors, a wide spectrum of patterns ranging from increased vascularity to total absence of perfusion in cases of tumor necrosis is observed. These perfusion patterns may be of some importance in patients receiving chemotherapy. In particular, the technique may be of some value in patients being contemplated for regional hepatic artery chemotherapy infusion, as optimum treatment response appears to be related to adequate tumor perfusion.[10]

Another approach for assessing the adequacy of regional hepatic artery infusion involves the direct injection of the hepatic artery catheter with Tc-99m microaggregated albumin or microspheres (MAM) particles followed by performance of a SPECT imaging study. This technique gives a very accurate assessment of the catheter tube position as well as the distribution of perfused liver parenchyma. Valuable information as regards tumor vascularity is also obtained with this examination.[11]

In addition, our preliminary experience is that the hepatic blood pool SPECT technique may be useful for evaluating the patency of the spleno-portal axis, mesenteric veins, inferior vena cava and the abdominal aorta. Finally, this technique has been shown to be of value for the detection of hepatic hemangiomata. In our experience, this approach represents a significant advance in the ability of the radionuclide blood pool technique to detect hepatic hemangiomata. Furthermore, examination time is reduced to less than 30 minutes for the SPECT study as compared to 3 hours for planar imaging.[12]

FUTURE DIRECTIONS

Future improvements in hepatic SPECT imaging will primarily involve the following areas: 1) development of new radiopharmaceuticals; 2) improved instrumentation, and 3) quantitation.

In the area of new radiopharmaceutical development, radiolabeled monoclonal antibodies appear to be promising. Early evidence suggests that SPECT imaging technology will be very important to the effective implementation of this imaging technique particularly in the liver as surrounding activity in normal structures may obscure disease. This approach appears to be applicable to a variety of diseases including a wide range of oncologic disorders. In the oncologic patient, the technique will be useful in defining presence, extent and follow-up of disease, and also in identifying the cases that would benefit the most from therapeutic doses of radiolabeled monoclonal antibodies.[13]

As a result of improving methods of attenuation correction, quantitation of functioning hepatic volume now appears somewhat more feasible. One particularly promising approach involves combining transmission and emission scanning techniques. The transmission study is performed first and is subsequently utilized to more accurately define attenuation variations throughout the liver (intrinsic method).[14] Such an approach should eventually result in more accurate quantitation of functioning hepatic volume.[15]

References

1. McAfee JG and Subramanian: Radioactive agents for imaging, in Freeman LM (ed.): Freeman and Johnson's Clinical Radionuclide Imaging. Orlando, Grune and Stratton, 1984, pp. 55-180.

2. Van Heertum RL, Brunetti JC, Yudd AP, et al: Liver SPECT. J Nucl Med Technol 13:236:241, 1985.

3. Strauss L, Bostel F, Clorius JH: Single-photon emission computed tomography (SPECT) for assessment of hepatic lesions. J Nucl Med 23:1059-65, 1982.

4. Croft BY, Teates CD: Experience with single photon emission computed tomography of the liver, in Esser PD (ed.) Emission Computed Tomography: Current Trends. New York, Society of Nuclear Medicine, 1983, pp. 155-62.

5. Keyes JW: Perspectives on tomography. J Nucl Med 23:633-640, 1982.

6. Khan O, Ell PJ, Javitt PH, et al: Comparison between emission and transmission computed tomography of the liver. Brit Med J 283:1212-1214, 1981.

7. Kudo M, Hirasa M, Takakuwa H, et al. Small Hepatocellular Carcinomas in Chronic Liver Disease: Detection with SPECT. Radiology 159(3):697-703, 1986.

8. Yudd AP, Van Heertum RL, Brunetti JC: Evaluation of Liver Disease: SPECT versus CAT. J Nucl Med 27:924, 1986.

9. Pettigrew RI, Witzum KF, Perkins GC, et al: Single photon emission computed tomograms of the liver: Normal vascular intra-hepatic structures. Radiology 150:219-223, 1984.

10. Kaplan WD, Dorsi CJ, Ensminger WD, et al: Intra-arterial radionuclide infusion: A new technique to assess chemotherapy perfusion patterns. Cancer 62:699-703, 1975.

11. Yang PJ, Thrall JH, Ensminger WD, et al: Perfusion scintigraphy (Tc-99m MAA) during surgery for placement of chemotherapy catheter in hepatic artery. Concise Communication. J Nucl Med 23:1066-1069, 1982.

12. Brunetti JC, Van Heertum RL, Yudd AP, et al: SPECT in the diagnosis of hepatic hemangioma. J Nucl Med 26:p8, 1985.

13. Larson SM, Carrasquillo JA, Reynolds JC: Radioimmunodetection and radioimmunotherapy. Cancer Investigation 2:363-81, 1984.

14. Malko JA, Van Heertum RL, Gullberg GT, et al: SPECT liver imaging using an iterative attenuation correction algorithm and an external flood source. J Nucl Med 27:701-705, 1986.

15. Strauss LG, Clorius JH, Frank T, et al: Single photon emission computerized tomography (SPECT) for estimates of liver and spleen volume. J Nucl Med 25:81-85, 1984.

NOTES

SPECT IN CLINICAL PRACTICE

Qualitative and Quantitative Hepatic SPECT Imaging

Harvey A. Ziessman, M.D.

Tc-99m macroaggregated albumin (Tc-MAA) hepatic arterial perfusion scintrigraphy has proven valuable in the clinical management of patients receiving intraarterial chemotherapy for primary and metastatic liver cancer (1-3). A good response to chemotherapy requires perfusion of the entire tumor-bearing liver. Extrahepatic perfusion can result in less drug delivered to the tumor as well as increased gastrointestinal and systemic exposure and toxicity. Overlying areas of intrahepatic and extrahepatic perfusion can sometimes make interpretation of these 2 dimensional images difficult (4,5). SPECT has the potential to depict the 3 dimensional distribution of perfusion, separate out overlying activity and improve contrast resolution.

We reviewed 91 SPECT Tc-MAA hepatic arterial perfusion studies (6) on patients with various cancers metastatic to the liver: colon (68), carcinoid (6), hepatoma (3), cholangiocarcinoma (3), pancreatic (2) and miscellaneous (4). All patients had angiography and planar Tc-99m Tc-SC liver-spleen scans. Twenty-six had SPECT Tc-SC studies.

The perfusion studies were performed by slowly injecting 4-6 mCi of Tc-MAA in 0.5 ml saline over 1 min through the subcutaneously implanted infusion pump sideport (Infusaid) or percutaneously placed hepatic arterial catheter, and then flushing with saline. Conventional 1000K count planar images were acquired in the ant, post, right and left lateral projections. A wide field of view gamma camera with a low energy all purpose parallel-hole collimator interfaced with a dedicated nuclear medicine computer was used. SPECT was performed by rotating the gamma camera about the patient's body in a 360 degree arc of 64 equally

spaced projections for 15 sec each. Tomographic images were reconstructed using filtered back-projection and modified 0.5 Ramp-Hanning filter. Attenuation correction was performed. The multiple-projection views were first viewed in rotating cine display and then the reconstructed transaxial, coronal and sagittal slices were examined. The planar Tc-MAA studies were initially interpreted prospectively over a 4 year period. At a later date they were reinterpreted retrospectively. The patient's Tc-SC study was always used for comparison. All SPECT Tc-MAA studies were then reviewed and interpreted. If a Tc-SC SPECT study was available, it was used for comparison, otherwise the planar study was used. The results of this comparison are shown below (6).

Extrahepatic abdominal perfusion (12%)

	Definite	Probable	Possible
Planar (prospectively)	5 *	2	
Planar (retrospectively)	5 *	3	5
SPECT	5 *	3	3

* 1 false neg.

Extrahepatic perfusion was confirmed by angiography in all patients with percutaneously placed catheters. In patients with surgically placed catheters, extrahepatic perfusion was seen again on at least 1 followup study. All patients with abdominal extrahepatic perfusion who received intraarterial chemotherapy through that catheter has symptoms of drug toxicity. Patients without evidence of extrahepatic perfusion had only a 23% incidence of similar symptoms ($p < .001$)

The rotating cine display was very useful in defining the three dimensional distribution of tumor and liver perfusion as well as

directing attention to areas of abdominal extrahepatic perfusion. Cross-sectional transaxial and coronal slices were particularly helpful in separating out gastric perfusion from overlapping perfusion of the liver, e.g. an enlarged left lobe. Importantly, SPECT improved our certainty in the interpretation of Tc-MAA perfusion scintigraphy.

In addition to providing improved qualitative information, SPECT has the potential for improved quantitative data compared to planar imaging. SPECT has enabled us to examine the in-vivo density of functional hepatic tumor microcirculation compared to that of normal liver (7).

Using the same protocal as described above, we analyzed discrete tumor nodules by reviewing each transaxial slice through the liver. The ratios between the Tc-MAA entrapment (and thus blood flow) in the center and the periphery of a tumor nodule and that in the adjacent uninvolved liver were obtained from profile histograms through the center of each discretely identifiable lesion. The orientation of the profile histogram was selected to encompass a portion of normal liver on either side of the lesion. The maximal count density in perfused portions of tumors was compared with the maximum in uninvolved liver tissue immediately adjacent to the metastatic lesions. Therefore, the perfusion to the vascular portions of the tumor relative to uninvolved liver was denoted by the count ratio of these respective regions. Tumor nodule size was determined using a profile histogram by measuring the maximum diameter of the nodule and width of the hypervascular rim.

Twenty-six liver tumor nodules were analyzed in 18 patients with metastatic colon cancer. Nodules equal to or greater than 9.5 cm in diameter appeared to have a cold hypoperfused center. The size of the central core was variable, but in all cases was surrounded by a rim of increased Tc-MAA activity. The size of the rim was less variable

(1.8-4.2 cm). In contrast, nodules < 8.5 cm in diameter did not have a hypovascular core and appeared solid. The greatest rim thickness in the ten largest nodules with diameters >9.5 cm was 4.2 cm. The maximum radius of the small solid nodules was 4.2 cm, probably indicating that the maximum depth to which tumor neovascularity can be generated from surrounding normal liver is approximately 4 cm. The ratio of Tc-MAA activity in tumor compared to normal adjacent liver tissue was always greater than one (median 2.7) and was unrelated to nodule size. Similar data was found in 14 carcinoid tumors, although the tumor to non-tumor perfusion ratio was slightly higher (4.4 mean). Three small nodules in a patient with hepatoma had tumor/non-tumor ratios of 20-30:1.

These results demonstrate that tumor nodules from both colorectal cancer and carcinoid are hyperperfused compared to adjacent uninvolved liver, and the pattern is dependent upon tumor size. This pattern correlates pathologically with the necrotic centers seen in large tumors. Although colon tumor nodules metastatic to the liver have been described in the past as hypovascular on celiac angiography, recent studies using superselective hepatic angiographic techniques have shown that nearly all hepatic metastases are hypervascular (8). These observations suggest that potentially exploitable differences between normal liver and hepatic tumor microcirculation exist and may ultimately enhance the potency of regional chemotherapy. Therapeutic effectiveness may be increased by efforts to focus therapy on the hypervascular portions of the tumor, where presumably active tumor prolifertion takes place. For example, radioactive microsphere therapy with Y-90 or P-32 could be administered intraarterially and deliver a 3-4 fold greater dose to tumor tissue than uninvolved liver. Therefore, SPECT quantitation may provide dosimetric data for intraarterial tumor radiotherapy.

Preliminary studies have shown the potential usefulness of SPECT for quantitating changes in tumor blood flow in response to intraarterially administered vasoconstrictors (9,10). Since tumor vascularity often lacks the normal smooth muscle layer sensitive to vasoconstrictors, an intraarterial infusion of a vasoconstrictor may produce relative shunting of blood toward tumor vessels and away from normal uninvolved adjacent tissue where the tissue vascularity is responsive to the drug's effect. This could further improve the tumor/non-tumor blood flow ratio, allowing increased preferential delivery of chemotherapy or radiotherapy to the tumor.

REFERENCES

1. Kaplan WD, Ensminger WD, et al: Radionuclide angiography to predict patient response to hepatic artery chemotherapy. Cancer Treat Rep 64:1217-1222, 1980

2. Yano PJ, Thrall JH, et al: Perfusion scintigraphy (Tc-99m MAA) during surgery for placement of chemotherapy cather in hepatic artery. J Nuc Med 23:1066-1069, 1982.

3. Bledin AG, Kantarjian HM, et al: ^{99m}Tc-labeled macroaggregrated albumin in intrahepatic arterial chemotherapy. AJR 143:321-325.

4. Ziessman HA, Thrall JH, et al: Hepatic arterial perfusion scintigraphy with Tc-99m-MAA. Radiology 152:167-172,1984.

5. Wahl RL, Ziessman HA, et al: Gastsric air contrast: useful adjunct tohepatic artery scintigraphy. AJR 143:321-325,1984.

6. Ziessman HA, Wahl RL, et al: The utility for SPECT for ^{99m}Tc-MAA hepatic arterial perfusion scintigraphy. AJR 145:747-751, 1985.

7. Gyves JW, Ziessman HA, et al: Definition of hepatic tumor microcirculation by single photon emission computerized tomography (SPECT). J Nucl Med 25:972-977,1984.

8. Chuang VP: Hepatic tumor angiography: A subject review. Rad 148:633-639,1983.

9. Ziessman HA, Gyves JW, et al: Atlas of hepatic arterial perfusion scintigraphy. Clin Nuc Med 10:675-681,1985.

10. Ziesman HA, Forastiere AA, et al:The use of a vasoconstrictor to improve tumour blood flow in intra-arterial chemotherapy: preliminary report. Nuc Med Comm 6:777-786,1985.

NOTES

SPECT IN CLINICAL PRACTICE

Functional Brain Imaging with Perfusion Tracers

Thomas C. Hill, M.D.

The rapid development of single-photon radiopharmaceuticals for cerebral blood flow study - which reveals function instead of morphology - has given new life to tomographic brain imaging in nuclear medicine. Progress in radiopharmaceuticals and refinements in neuro-SPECT instrumentation are helping to reinstate brain scintigraphy as an important part of neurologic diagnosis.

Single-photon emission computed tomography of the brain evolved from experimentation using prototype instrumentation during the early 1960s. Although tomographic studies provided superior diagnostic accuracy when compared to planar techniques, the arrival of x-ray CT of the head resulted in the rapid demise of technetium brain imaging. Both methods provided anatomic delineation of blood-brain barrier abnormalities.

Some clinical value for SPECT was demonstrated by Kuhl, Budinger, Keyes and others in the 1960s and early 70s. [1,2,3] When commercial instruments became available in the late 1970s, the sensitivity and specificity of SPECT was compared to state-of-the-art radionuclide scintigraphy with Anger cameras and transmission tomography.[4]

Using the Cleon-710 dedicated SPECT system with technetium agents, one study of 235 patients yielded a sensitivity of 77% with specificity of 99% -

an improvement of about 10% over the diagnostic accuracy of planar imaging with an Anger camera.[5] The tomographic images differentiated superficial abnormalities from deep intracranial lesions, demonstrated cerebral metastases that were not visible on radionuclide scintigraphy or transmission tomography, and showed an isodense subdural hematoma. The overall accuracy of transmission tomography was similar to the SPECT study. Other early studies comparing planar imaging and ECT had similar results but the rapid expansion of x-ray CT soon rendered radionuclide studies of the brain obsolete.

The term "conventional brain scanning" has often been inappropriately applied in nuclear medicine. Conventional brain scanning is actually non-brain imaging using radiopharmaceuticals such as Tc-99m pertechnetate, which do not penetrate normal brain but will cross a damaged blood-brain barrier to create focal areas of increased activity in regions of brain pathology. Tc-99m-DPTA was introduced to allow earlier imaging than is possible with Tc-99m-pertechnetate, while achieving similar clinical results.

The principal factors that influence radiopharmaceutical localization in brain tumors are vascularity, interstitial fluid, capillary permeability and intracellular uptake.[6] The superiority of Tc-99m-glocoheptonate in brain localization was suggested to many investigators to reflect a different mechanism of localization in tumors when compared to other brain scanning agents.[7] Good single-photon tracers were needed for radionuclide brain imaging to flourish, however. These radiopharmaceuticals can reveal

functional processes and thus complement rather than compete with transmission tomography and its anatomic information.

Enthusiasm for SPECT of the brain has been stimulated by the success of positron emission tomography, although the method has been limited by slow development of practical single-photon radiopharmaceuticals. The annihilation reaction with coincidence counting of positron isotopes of carbon, oxygen, nitrogen and fluorine is intrinsically ideal for studying metabolic pathways in the brain.

The clinical utility of PET is limited, however, because of the need for costly on-site cyclotrons and the technical support of radiochemical and pharmaceutical production. If the dramatic results obtained from work at current PET centers is to be repeated in general clinical settings, single-photon radiopharmaceuticals that are free of high technology costs and that can mimic the biologic distribution of positron pharmaceuticals are required. Widespread clinical utility would then be limited only by the cost of instrumentation.

Regional brain perfusion can be demonstrated with dynamic imaging and equilibrium flow imaging with diffusible or extractable tracers.[8] Stokely et al. have shown that dynamic flow imaging is clinically feasible with single-photon tomography.[9] Fazio et al. have demonstrated that equilibrium imaging with short-lived pharmaceuticals can produce images that reflect regional brain perfusion and demonstrate physiologic deviations from

normal brain perfusion.[10] The extractable tracer approach appears to be better suited for widespread use in nuclear medicine, however. Pharmaceuticals that are lipid-soluble and have a high extraction fraction on the first pass through the brain - such as N-isopropyl iodoamphetamine (IMP) and I-123 HIPDM - fit into this latter category.

Iodine-123 IMP is extracted rapidly by the brain with about 7%of the injected dose reaching that organ within 20 minutes of intravenous injection. The initial distribution of the tracer is proportional to cerebral blood flow.[12] I-123 IMP remains trapped within the brain with little change in its distribution for at least an hour. As a result, SPECT can be performed with either special purpose instrumentation such as the scanning multi-detector system developed by Cleon or the rotating gamma camera.

The most promising use of the technique at present is in patients with suspected acute cerebral infarction.[13-15] Unless the infarction is due to hemorrhage, the CT scan will usually be normal for several days after the initial symptoms. I-123 IMP imaging, on the other hand, will be abnormal immediately. Our earliest documented I-123 IMP study was obtained four hours after onset of symptoms and demonstrated a large perfusion defect in an area that was initially normal on CT examination and that became abnormal only after several days.

I-123 IMP imaging is highly sensitive for detecting perfusion defects in patients with stroke. With good technique, I-123 IMP imaging can reliably detect the distribution of the major cerebral vessels and infarction limited to the basal ganglia and the cerebellar hemispheres.

The early detection of stroke has previously been of limited value because there was no satisfactory therapy to reverse its effects. But there has been a dramatic shift in medical therapy.[16] Stroke is a continuing process frequently preceded by rapidly progressing symptoms probably due to a series of ministrokes. A number of surgical therapies, including temporal artery bypass surgery, have been proposed to salvage as much reversibly ischemic cerebral tissue as possible. Medical therapies such as hemodilution, lysis, oxygen-carrying fluorocarbons and calcium channel blocker therapy promise to change the way we treat patients with impending stroke. For these reasons, it is critical that the presence and extent of a perfusion defect be detected as early as possible.

Preliminary studies using I-123 IMP SPECT suggest how the application of this technique in early stroke might be used to stratify patients. Lee et al. have observed a relationship between prognosis and the extent of the initial perfusion defect.[17] Patients with minimal perfusion defects had total or near total recoveries by six months after the stroke. On the other hand, half the patients with large perfusion defects had no or minimal recoveries. The early identification of these patients and the prompt institution of aggressive therapy could potentially salvage many patients whose outcomes are bleak with conventional therapy.

The value of early identification in patients with stroke suggests the need to identify hemodynamically significant arterial stenoses before infarction. This will be more difficult since the sensitivity of I-123 IMP imaging in patients with previous TIAs is low. Coupling this method with interventions such as hyperventilation, carbon dioxide inhalation or increasing cerebral blood flow with Diamox may improve its sensitivity. Supplementing the perfusion information with blood pool images may also be helpful.

Another important role for I-123 IMP SPECT will be in the assessment of patients with suspected Alzheimer's disease. While understanding of this disease has mushroomed in the past decade, diagnosis still depends on clinical examination and psychometric testing; therapeutic interventions are only in their infancy. Progress in clinical diagnosis has been hampered by the absence of in vivo tests that accurately separate Alzheimer's disease from other forms of dementia.

In vivo imaging of cerebral blood flow and regional glucose utilization using PET has succeeded in defining regional abnormalities in patients with Alzheimer's disease and normal CT studies. While the metabolic rate is decreased throughout the brain, the most severely affected area is in the parietal cortex.

SPECT studies of the brain using I-123 IMP have also shown a marked reduction in tracer uptake in the posterior temporal and parietal regions in patients with Alzheimer's disease.[18] The perfusion defects are bilaterally symmetric. As the disease progresses, tracer uptake is reduced over a greater extent of the brain, extending anteriorly into the temporal and frontal lobes. The extension may be asymmetrical but sparing the primary motor and sensory strips along the Rolandic fissure, the primary visual cortex, the basal ganglia and the cerebellum.

Other forms of dementia produce patterns that are easily distinguished from Alzheimer's disease. Thus, patients with multi-infarct dementia have multiple perfusion defects distributed symmetrically throughout the brain. Patients with Parkinson's disease have perfusion patterns similar to normal age-matched controls. The dementia accompanying multiple sclerosis results in a frontal lobe syndrome and a corresponding decrease in tracer uptake in the frontal lobes. Normal pressure hydrocephalus results in bilaterally symmetrical reductions in tracer uptake limited to the paraventricular areas and extending, in severe cases, to the frontal cortex.

Functional imaging with I-123 IMP appears sensitive to detecting and assessing Alzheimer's disease even in its mild to moderate stages. The accuracy of the method has had only preliminary study, however, particularly in patients with the earliest stages of the disease prior to the development of significant clinical signs and symptoms.

To obtain optimal SPECT imaging with I-123-labeled amines, high purity I-123 made from the p,5n method of production will be needed. Even with the p,2n methods of production, the limited availability of I-123 may prevent routine use of these iodinated perfusion agents.

Technetium-99m propyleneamine oxine (PNAO) and its derivatives have been developed by Volkert and Holmes.[19] Early derivatives of these lipophilic compound crossed the blood brain barrier but cleared very rapidly from the brain, which precluded tomographic imaging.[20] Improvements in brain residence time have been accomplished with newer HMPAO derivatives.[21]

Technetium-99m-labeled 1,2 dithio-5-8 diazocyclodecane (BAT) has a more favorable residence time in the brain (half-life of 102 minutes). When tomographic studies were performed in the monkey with this agent, however, the images failed to clearly differentiate between gray and white matter. Initial BAT distribution is proportional to cerebral blood flow, but the pharmaceutical redistributes within the brain by 15 minutes and thus poorly differentiates gray and white matter.[22]

Thallium-201 diethyldithiocarbamate (DDC) has also been described as an alternative to I-123 iodoamphetamine.[23] Development of this imaging agent followed the observation that treating thallium intoxication with large doses of diethyldithiocarbamate had increasing neurologic toxicity. Although thallium-201 is not ideal for SPECT imaging, its availability and the ease with which it can be complexed with DDC make it an attractive alternative to iodinated amines.

When injected intravenously, the biodistribution of TI-201 DDC is similar to TI-201 chloride with the exception of brain uptake. Tomographic images obtained after intravenous injection of the tracer show high gray matter uptake and look similar to images obtained with I-123 IMP. The TI-201 DDC stays in the brain longer that I-123 IMP and yields good gray matter-white matter differentiation up to 24 hours after injection.

Ultimately, a Tc-99m-labeled tracer will be necessary for cerebral perfusion imaging to achieve a high level of clinical acceptance. The commercial distribution and high cost of I-123-labeled agents will make the agent uncompetitive with a Tc-99m agent that can be prepared routinely from a kit, provided the Tc-99m-labeled agent provides images of comparable quality. Experience with I-123-labeled amines, nevertheless, provide clinicians with the tools necessary to forge the new field of clinical cerebral perfusion imaging. Furthermore, Tc-99m-labeled brain perfusion agents will likely not be commercially available in the U.S. before the 1990s.

Promising areas for future clinical investigation have already begun to be redefined by work at positron tomographic centers. For example, the metabolic brain response to cognitive input varies regionally among different populations.[24] This work has important clinical implications in the field of educational psychology and in dealing with learning disabilities. Do patients with specific learning disabilities process input stimuli in

different regions than the normal population. Does special education change these regional responses? Answers to these questions would have important implications in the diagnosis and treatment of learning disabilities.

In psychiatric disorders, PET studies have demonstrated regional differences in metabolism between psychosis in schizophrenia and manic depressive illness. Changes gave also been observed in unipolar and bipolar depression. Functional tests of regional perfusion may have critical importance for monitoring the recovery of mentally ill patients under the effects of various dugs. [25] These observations, made with the aid of positron techniques, are likely to be duplicated with SPECT and iodinated amines. SPECT methods are far from monitoring the recovery of mentally ill patients under the effects of various drugs. [25] These observations, made with the aid of positron techniques, are likely to be duplicated with SPECT and iodinated amines. SPECT methods are far more likely to move these diagnostic and therapeutic possibilities into clinical realities. Single-photon techniques using receptor-specific radiotracers such as those described by Eckelman and co-workers should yield even more precise pathophysiologic information that blood flow or metabolism information alone. [26]

References

1. Kuhl DE, Edwards RQ: Image separation radioisotope scanning. Radiology 80:653-661, 1963.

2. Budinger T, Gulberg GT: Three-dimensional reconstruction in nuclear medicine by iterative least-squares and Fourier transform techniques. IEEE Trans Nucl Sci NS-21:2-10, 1974.

3. Keyes JW Jr, Orlandea N, Heetderks WT, et al.: The humongotron - a scintillation-camera transaxial tomography. J Nucl Med 18:381-387, 1977.

4. Hill TC, Costello P, Gramm HF, et al.: Early clinical experience with a radionuclide emission computed tomographic brain imaging system. Radiology 128:803-806, 1978.

5. Hill TC, Lovett RD, McNeil BJ: Observations on the clinical value of emission tomography. J Nucl Med 21:613-616, 1980.

6. Tutor CH: Radiopharmaceuticals for tumor localization with special emphasis on brain tumors. In: Radiopharmaceuticals, G. Subravianian, B.A. Rhodes, J.F. Cooper, U.T. Sodd, eds. New York Society of Nuclear Medicine, pp. 474-481, 1975.

7. Waxman AB, Tanasercu AA, Siemsen JK, et al.: ^{99}mTc-glucoheptonate as a brain scanning agent. Critical comparison with pertechnate. J Nucl Med 17:345-348, 1976.

8. Budinger TF, Gullberg GT, Huesman RH: Emission computed tomography. Chapter 5. In: Image Reconstruction from Projections, Implementation and Applications, Vol 32: Topics in Applied Physics. Herman GT, Ed. New York, Springer Verlag, 1979, pp. 147-246.

9. Stokely EM, Sveinsdottir E, Lassen NA, et al.: A single photon dynamic computer assisted tomograph (DCAT) for imaging brain function in multiple cross sections. J Comput Assist Tomogr 4:230-240, 1980.

10. Fazio F, Fleschi C, Collice M, et al.: Tomographic assessment of cerebral perfusion using single-photon emitter krypton-81m and a rotating gamma camera. J Nucl Med 21:1139-1145, 1980.

11. Winchell HS, Horst WD, Braun L, Ildendorf WH, Hattner R, Parker H: N-isopropyl-[I-123] p-iodoamphetamine: Single-pass brain uptake and washout: binding to brain synaptosomes; and localization in dog and monkey brain. J Nucl Med 21:947-952.

12. Kuhl DE, Barrio JR, Huang S-C, Selin C, Ackermann RF, Lear JL, Wu JL, Lin TH, Phelps ME: Quantifying local cerebral blood flow by N-isopropyl-p^{123}I iodoamphetamine (IMP) tomography. J Nucl Med 23:196-203, 1982.

13. Hill TC, Holman BL, Lovett R, O'Leary DH, Front D, Magistretti P, Zimmerman RE, Moore SC, Clouse ME, Wu JL, Lin TH, Baldwin RM. Initial experience with SPECT of the brain using N-isopropyl I-123 p-iodoamphetamine. J Nucl Med 23:191-195, 1982.

14. Holman BL, Hill TC, Polak JF, Lee RGL, Royal HD, O'Leary DH: Cerebral perfusion imaging with I-123 labeled amines. Arch Neurol 41:1060-1066, 1984.

15. Hill TC, Magistretti PL, Holman BL, Lee RGL, O'Leary DH, Uren RF, Royal HD, Mayman CL, Kolodny GM, Clouse ME: Assessment of regional cerebral blood flow (rCBF) in stroke using SPECT and N-isopropyl (I-123)-p-iodoamphetamine (IMP). Stroke 15:40-45, 1984.

16 Foreman J: Quick action in limiting damage from stroke. Boston Globe p. 45, April 15, 1985.

17. Lee RGL, Hill TC, Holman BL, Royal HD, Clouse ME: The predictive value of perfusion defect size using N-isopropyl I-123 p-iodoamphetamine emission tomography in acute stroke. J Neurosurg 61:449-452, 1984.

18. Mueller SP, Johnson KA, Hamil D, English RJ, Nagel SJ, Ichise M, Holman BL: Assessment of I-123 IMP SPECT in mild/moderate and severe alzheimer's disease. J Nucl Med 27:889, 1986 (abstr).

19. Volkert QA, McKenzie E, Hoffman TJ, Troutner DE, Holmes RA: Effects of ligand structure on the lipophilicity and biodistribution of Tc-99m amine oxine chelates. J Nucl Med 25:15, 1984 (abstr).

20. Hill TC, Moore SC, Volkert WA, Holmes RA, Kung HF, Blau M, Mueller S, Holman BL, Clouse ME: SPECT imaging of technetium lipophilic brain agents. Eur J Nucl Med 9:A374, 1984.

21. Podreka I, Suess E, Goldenberg G, Steiner M, Brucke T, Muller C, Deecke L: Initial experience with Tc-99m-Hexamethylpropyleneamine oxime (Tc-99m-HMPAO) brain SPECT. J Nucl Med 27:887-888, 1986 (abstr).

22. Kung HF, Yu CC, Billings J, Molnar M, Wicks R, Blau M: New Tc-99m brain imaging agents. J Nucl Med 25:P16,1984. (abstr.).

23. Bruive JF, VanRoyer EA, Vyth A, DeJong JM, Van der Schoot JB: Tl-201-diethyldithiocarbamate: An alternative to I-123 IMP. J Nucl Med (in press).

24. Phelps ME, Mazziotta JC, Carson RE, et al.: Human cerebral metabolic responses to verbal and nonverbal auditory stimulation measured with positron computed tomography. J Nucl Med 23:6, 1982 (abstr).

25. Widew L, Blomquist T, Greitz T, et al.: PET studies of glucose metabolism in patients with schizophrenia. AJNR 4:550-552, May/June 1983.

26. Eckelman WC: In Ell PJ, Holman BL (eds): Receptor Specific Radiopharmaceuticals in Computed Emission Tomography. Oxford, England, Oxford University Press, 1982.

NOTES

SPECT IN CLINICAL PRACTICE

Dynamic Brain Imaging with SPECT

Michael D. Devous, Sr., Ph.D.

Single-photon emission computed tomography (SPECT) is a rapidly developing technology capable of making 3-dimensional measurements of cerebral physiology. Recent developments in radiopharmaceuticals and imaging instruments have made SPECT competitive with positron emission tomography (PET) in many aspects of functional brain imaging. It is now possible to make detailed measurements of regional cerebral blood flow (rCBF) and receptor function with instruments and radiopharmaceuticals that are pratical for routine clinical application.

The value of SPECT is that it offers the potential to image brain biochemical processes (particularly blood flow) that are directly related to neuronal activity and thus to cognition. It has long been recognized that many neurologic and psychiatric disorders are not associated with a structural lesion. Therefore, many investigators have attempted to develop tools by which brain function, rather than structure, can be assessed. Chief among these has been the measurement of brain blood flow because of its important role in providing nutrients and because of its autoregulatory link to brain metabolism. The measurement of whole-brain blood flow in humans was first reported in 1948 by Kety and Schmidt. Their technique was rapidly expanded to include the use of

radioactive materials as the inert tracers, and to include measurements of regional blood flow by using numerous radiation detector probes placed about the head.

Two-dimensional measurements were limited in that they reflected changes in flow occurring primarily on the brain surface, while disorders in brain physiology associated with deep structures, such as basal ganglia, were impossible to observe. During the development of 2-dimensional methods for assessing brain function, 3-dimensional methods for measuring internal structure were also being developed. The concept of tomography (deriving 3-dimensional information from 2-dimensional data) takes its roots from the solution of a mathematical problem in astronomy presented by Radon at the turn of the century. Kuhl and Edwards (1963) were the first to apply tomographic principles to reconstruct 3-dimensional images of the distribution of radiotracers in humans, which ultimately led to the technologies we now call SPECT and PET.

It was the marriage of 3-dimensional imaging technology with radiotracer measurements of rCBF that permitted the first views of physiologic behavior of the brain beneath the cortical surface. Three tomographic technologies have been employed to measure rCBF: x-ray CT, PET and SPECT. Most cost-effective of these may be SPECT, particularly given recent radiopharmaceutical and instrumentation developments.

The first successful tomographic imaging of rCBF with diffusible noble gas indicators was by Yamamoto and colleagues (1977) employing

Krypton-77 and PET imaging. Drayer et al (1978) successfully utilized stable Xenon inhalation with x-ray CT to calculate rCBF and Xenon partition coefficients from observed density changes. Drs. Ernest Stokely of our group and Niels Lassen of Copenhagen designed the first SPECT device to measure rCBF by monitoring the cerebral transit of inhaled Xe-133.

Newer SPECT systems such as rotating gamma cameras are too slow and too insensitive to measure rCBF by monitoring cerebral transit of an inert radiotracer. Fortunately, new radiopharmaceuticals have been designed which can be given intravenously and which distribute to the brain in proportion to rCBF. These "static" radiopharmaceuticals (I-123 IMP, I-123 HIPDM, Tc-99m HM-PAO and Tc-99m NEP-DADT) are much like fluorodeoxyglucose used for PET metabolism imaging in that once they arrive in the brain they are retained for a period ranging from 40 minutes to several hours. This permits less sensitive, slower machines to obtain moderate-resolution rCBF images. Most recently, a collaborative effort between industry and our laboratory has led to the development of a SPECT system (TRIAD) capable of high-resolution imaging of statically distributed radiopharmaceuticals and quantitative measurements of dynamic radiopharmaceuticals such as Xe-133 (see for example Lim et al, 1985).

The distinction between "dynamic" and "static" radiopharmaceuticals is an important one. Dynamic measurements occur over a short period of time and reflect cerebral physiology at the time of the measurement in quantitative terms. Such quantitative measurements are valuable in that

they allow intercomparison among patients and among studies for the same patient across time. Dynamic SPECT also permits repeat studies within a few minutes so that rapidly changing environments, such as responses to drug interventions, can be monitored. The rapid imaging required for dynamic measurements minimizes count densities and thus such systems trade resolution for sensitivity. The original system developed by Stokely et al for Xe-133 SPECT had very high sensitivity but a resolution of only 17 mm.

Static radiopharmaceuticals labeled with Tc-99m or I-123 are fixed in brain tissue for periods of time long enough to use high-resolution low-sensitivity collimation and still acquire adequate count densities for good imaging. Such techniques will yield a better anatomic correspondence between rCBF measurements and structural entities. In addition, imaging can occur at some time after the physiologic event since the images reflect brain behavior at the time of radiopharmaceutical injection. For example, a seizure patient could be injected with a brain radiopharmaceutical during ictus, and imaged after the seizure is controlled. The disadvantages of "static" agents are that studies cannot be repeated for at least 24 hours and the data obtained are not quantitative. Efforts are underway to model the distribution of "static" radiopharmaceuticals in order to convert the resulting images to quantitative measurements but these have not yet been successful.

The rCBF images shown in this presentation were obtained with the Tomomatic 64 (Medimatic A/S, Copenhagen, Denmark) designed by

Dr. Ernest Stokely in our laboratory. The total study time is 4 minutes and quantitative rCBF images are displayed in a color scale in ml/min/100 g. Three transverse cross-sectional images each separated from the other by 4 cm are obtained 2, 6 and 10 cm above and parallel to the cantho-meatal line. The results of such imaging in normal volunteers have been presented by Devous et al (1986). Average gray-matter flow is on the order of 70 ml/min/100 g and is very symmetric. Highest flows are generally seen in the parietal lobes, except for the subregion of the occipital lobe containing the visual cortex which has very high flows when patients are studied with their eyes open. RCBF declines slightly with age and is higher in females than males at all ages.

There are several advantages to dynamic SPECT, including:

--Radiation dosimetry is favorable, permitting multiple studies in the same patient.

--The procedure takes only 4 minutes so that studies can be conducted in severely disturbed patients.

--It is non-invasive and repeatable within 15 minutes.

--Tomographic imaging permits analyses of deep-lying structures.

--It is responsive to cognitive tasks, sensory stimulation and pharmacologic activation.

--It is relatively inexpensive and can be performed in typical hospital nuclear medicine facilities.

Dynamic SPECT has been employed in our laboratory to measure rCBF in normal volunteers and in numerous patient populations. These include cerebral vascular disease and stroke, seizure disorders, dementia, neurosurgical complications such as arteriovenous malformations and subarachnoid hemorrhage, affective disorders, schizophrenia, dyslexia, speech pathology, hypertension, and other pathologies which may not have their principal features associated with the central nervous system. Although these studies have been performed with a prototype unit, they illustrate the utility of SPECT brain imaging independent of the instrumentation or radiopharmaceutical employed. It has become clear that the widespread availability and affordability of SPECT will make it possible for functional brain imaging to enter the regimen of routine nuclear medicine procedures. Alterations in rCBF distributions subsequent to administration of psychoactive medications, vasodilators, or cognitive tasks could provide a powerful discriminant for diagnosis or prognosis. In addition, radiopharmaceuticals for SPECT measurement of various receptor systems are rapidly being developed. Their use should provide further measures of brain function in important patient populations. Finally, the value of functional brain imaging in various patient populations for whom structural brain imaging is uninformative may return the brain scan so popular prior to the CT era to a place of prominance in nuclear medicine.

GENERAL REFERENCES

Dynamic SPECT Technique:

Kety SS, Schmidt CF: The nitrous oxide method for quantitative determination of cerebral blood flow in man: Theory, procedure and normal values. J Clin Invest 27:475-483, 1948

Lassen NA, Ingvar DH, Skinhøj E: Brain function in blood flow. Sci Am 239:62-71, 1978

Devous MD Sr, Stokely EM, Bonte FJ: Quantitative imaging of regional cerebral blood flow in man by dynamic single-photon tomography. In: Radionuclide Imaging of the Brain. BL Holman, Editor. Churchill-Livingstone, pp 135-162, 1985

Drayer PP, Wolfson SK, Reinmuth OW, et al: Xenon enhanced CT for analysis of cerebral integrity, perfusion and blood flow. Stroke 9:123-126, 1978

Yamamoto YL, Thompson CJ, Meyer E, et al: Dynamic positron emission tomography for study of cerebral hemodynamics in a cross-section of the head using positron-emitting 68-Ga-EDTA and 77-Kr. J Comput Assist Tomogr 1:43-56, 1977

Instrumentation:

Kuhl DE, Edwards RQ: Image separation radioisotope scanning. Radiol 80:653-662, 1963

Stokely EM, Sveinsdottir E, Lassen NA, Rommer P: A single-photon dynamic computer-assisted tomograph (DCAT) for imaging brain function in multiple cross-sections. J Comput Assist Tomogr 4:230-240, 1980

Lim C, Gottschalk S, Walker R, et al: Triangular SPECT system for 3-D total organ volume imaging: Design concept and preliminary imaging results. IEEE Trans Nucl Sci NS-32/1:741-747, 1985

Applications:

Bonte FJ, Devous MD Sr, Stokely EM, Homan RW: Single-photon tomographic determination of regional brain blood flow in epilepsy. AJNR 4:544-546, 1983

Bonte FJ, Stokely EM, Devous MD Sr: Single-photon emission computerized tomography of regional cerebral blood flow in cerebrovascular disease and stroke. Noninv Med Imag 1:9-16, 1984

Devous MD Sr, Bonte FJ, Stokely EM: The normal distribution of regional cerebral blood flow measured by dynamic single-photon emission tomography. J Cereb Blood Flow Metab 6:95-104, 1986

Homan RW, Devous MD Sr, Stokely EM, Bonte FJ: Quantification of intracerebral steal in patients with arteriovenous malformations. Arch Neurol 43:779-785, 1986

Reed WG, Devous MD Sr: Cerebral blood flow autoregulation and hypertension. Am J Med Sci 289:37-44, 1985

Devous MD Sr, Raese JD, Herman JH, et al: Regional cerebral blood flow in schizophrenic patients at rest and during Wisconsin Card Sort task. J Cereb Blood Flow Metab 5:S201-S203, 1985

Bonte FJ, Ross ED, Chehabi HH, Devous MD Sr: SPECT study of regional cerebral blood flow in Alzheimer's disease. J Comput Assist Tomogr 10:579-583, 1986

NOTES

SPECT IN CLINICAL PRACTICE

SPECT in the Quantitative Imaging of Radiolabeled Antibodies

Peter Leichner, Ph.D.

Clinical experience in the treatment of diverse cancers with I-131 labeled antibodies to date has demonstrated encouraging results (1-4), and additional clinical trials in radioimmunotherapy with a variety of new antibodies and new radiolabels have begun or are about to commence. A series of dosimetric studies (5-7) has shown that quantitation of the activity of radiolabeled antibodies in target tumors and normal tissues in conjunction with radiation absorbed-dose estimates provides a foundation for choosing among antibodies, methods of infusion, and activities to be administered to optimize this new treatment modality. Progress in bifunctional chelation chemistry has led to the development of In-111 and Y-90 labeled antibodies, and dosimetric data for Y-90 antiferritin in the treatment of hepatoma have recently been reported (8). These developments in radiolabeled antibody technology present new challenges and opportunities for the field of nuclear medicine, especially in the area of treatment planning for radioimmunotherapy.

For example, treatment planning for Y-90 antiferritin for patients with hepatoma includes measurements of the uptake and clearance of In-111 antiferritin in the target tumor and normal liver from serial scintillation camera images, hepatoma and normal liver volumetrics (currently computed from CT scans), and radiation dose estimates based on these data. Additionally, increasing reliance has been placed on SPECT imaging in clinical decision making because transverse slices reveal details about tumor targeting that are difficult, if not impossible, to visualize in planar scintillation camera images.

For I-131 antiferritin in hepatoma, dual-energy SPECT, with Tc-99m sulfur coloid as the second imaging agent, was determined to be of considerable clinical advantage because both radionuclides were imaged in a single rotational acquisition and reconstructed slices matched exactly. Tumor targeting of antiferritin could, therefore, be demonstrated more rapidly and definitively than would otherwise have been possible. Similarly, In-111 antiferritin is being imaged in the dual-energy mode, and transverse slices are compared to the corresponding Tc-99m sulfur colloid study (acquired separately). In a series of phantom studies it was determined that 128 views in a rotational acquisition resulted in better hot lesion detectability than 64 views. In our current imaging protocol for clinical

studies, patients are administered 3-4 mCi of In-111 antiferritin, labeled at approximately 7 mCi per mg of IgG, and liver imaging is carried out in 128 angular intervals, with an acquisition time of 15 seconds per view. Including set-up time, about 40 minutes are required for each tomographic study.

The clinical advantages of SPECT imaging in radioimmunotherapy have included the following:tumor localization of radiolabeled antibodies is more easily visualized in transverse slices than in planar views, necrotic regions within large tumors may be detected with relative ease, and tumor-to-normal tissue ratios may be determined more reliably from SPECT slices than from planar views. These are important parameters that influence treatment decisions, and as SPECT instrumentation and reconstruction algorithms continue to improve, SPECT imaging will play an increasingly important role in radioimmunotherapy treatment planning.

REFERENCES

1. Larson, S.M., Carrasquillo, J.A., Krohn, K.A., Brown, J.P., McGuffin, R.W., Ferens, J.M., Graham, M.M., Hill, L.D., Beaumeier, P.L., and Hellstrom, K.E. Localization of I-131 labeled p-97 specific Fab fragments in human melanoma as a basis for radiotherapy. J. Clin. Invest. 72:2101 -2114, 1983.

2. Carrasquillo, J.A., Krohn, K.A., Beaumeier, P.L., McGuffin, R.W., Brown, J.P., Hellstrom, K.E., Hellstrom, I., and Larson, M. Diagnosis of and therapy for solid tumors with radiolabeled antibodies and immune fragments. Cancer Treat. Rep. 68:317-328, 1984.

3. Epenetos, A.A., Helnan, K.A., Hooker, G., Hughes, J.M.B., Krausz, T., Lavender, J.P., MacGregor, W.G., et al. Antibody-guided irradiation of malignant lesions: three cases illustrating a new method of treatment. Lancet No. 8392:1441-1443, 1984.

4. Order, S.E., Stillwagon, G.B., Klein, J.L., Leichner, P.K., Siegelman, S.S., Fishman, E.K., Ettinger, D.S., Haulk, T., Kopher K., Finney, K., Surdyke, M., Self, S., Leibel, S. Iodine 131 Antiferritin, a new treatment modality in hepatoma: a radiation therapy oncology group study. J. Clin. Oncol. 3: 1573-1582, 1985.

5. Leichner, P.K., Klein, J.L., Garrison, J.B, Jenkins, R.E., Nickoloff, E.L., Ettinger, D.S., and Order, S.E. Dosimetry of I-131 labeled antiferritin in hepatoma: a model for radioimmunoglobulin dosimetry. Int. J. Radiation Oncology Biol. Phys.7:323-333, 1981.

6. Leichner, P.K., Klein, J.L., Siegelman, S.S., Ettinger, D.S., and Order, S.E. Dosimetry of I-131 labeled antiferritin in hepatoma: specific activities in the tumor and liver. Cancer Treat. Rep. 67:647-658, 1983.

7. Leichner, P.K., Klein, J.L., Fishman, E.K., Siegelman, S.S., Ettinger, D.S., and Order, S.E. Comparative tumor dose from I-131 labeled antiferritin, anti-AFP, and anti-CEA in primary liver cancers. Cancer Drug Del.1:321-328, 1984.

8. Order, S.E, Klein, J.L., Leichner, P.K., Frincke, J. Lollo, C., and Carlo D.J. Y-90 antiferritin - a new therapeutic radiolabeled antibody. Int. J. Radiation Oncology Biol. Phys. 12:277-281, 1986.

NOTES

SPECT IN CLINICAL PRACTICE

SPECT Imaging of the Thorax: Emphasis on Ga-67 for Tumor and Infection

Naomi P. Alazraki, M.D.

PHANTOM STUDIES:

Planar imaging with Gallium 67 has always been complex and difficult, and SPECT further complicates those problems. To determine the best SPECT imaging parameters for gallium 67, we have done studies using a chest phantom, with lesions of 1.5cm x 1cm and 2.2cm diameter placed in the center of the phantom to simulate mediastinal tumors (1). Lesion to background ratios were varied between 5:1 and 30:1. Images were performed using the following pulse-height-analyzer settings: 184 KeV alone, dual peaks 184 and 296 KeV, and triple peaks 93, 184, and 296 KeV windows. 360° acquisitions were obtained and reconstructions were performed using all 64 images over 360°, or 32 images over 180°, with varying choices of the 180° arc selection. As part of the phantom, a simulated sternum, 3.5x1cm rectangular tube - 17cm long containing a lesion to background activity ratio of 3.7:1, and a simulated spine, a 2.2cm diameter x 17cm length tube containing a lesion to background activity ratio of 3.7:1, were also imaged in the phantom studies. The results indicated that the 360° acquisition was necessary, since although in some instances the 180° acquisition actually gave superior resolution for centrally placed lesions, often superficial structures (the

sternum and spine) and potentially peripheral lesions were not visualized depending upon the choice of the arc. Central lesions were detectable at 10:1 lesion to background ratios, but not at 5:1. For the collimator and camera used in these studies, the 184 and 296 KeV dual peak images gave best imaging results, although the 184 KeV peak alone was equally good. Superficial structures including the sternum and spine were better seen than the deep lesions on the 360° acquisitions even though lesion to background ratios were lower. Long lesions were better seen than short ones. Attenuation corrections did not improve the images.

LUNG CANCER - MEDIASTINAL LESIONS

Correlative studies between gallium mediastinal lesion detection and CT of the chest in staging patients with lung cancer have shown that CT is superior (2). The studies, however, to date have mainly compared planar gallium imaging to CT of the chest. The improved resolution of SPECT imaging compared to planar imaging raises the question of how much improvement in this clinical problem we can expect from SPECT (see attached discussion on Staging Lung Cancer). O'Donnell, studying this problem at the Cleveland Clinic, claims excellent results for SPECT gallium compared with CT (3).

STERNAL OSTEOMYELITIS

Another clinical area where SPECT imaging has contributed to

clinical diagnosis is sternal osteomyelitis vs sub-sternal mediastinitis in patients following coronary artery bypass surgery. SPECT imaging of the gallium uptake in the sternum and sub-sternal regions provides a tool for differentiating between mediastinitis, osteomyelitis, and cellulitis. In-111 labeled leukocytes would also be a satisfactory agent for evaluating this problem.

TECHNIQUE

At the Salt Lake VA Medical Center, our current protocol for SPECT Gallium 67 imaging includes: 7.5mCi of Ga-67 citrate administered approximately 72 hours prior to imaging. The 184 and 296 KeV peaks or all three peaks are used, depending upon the collimator and camera used. A 360° acquisition of 64 images acquired for 60 seconds each on a 64x64 matrix is performed. Processing involves uniformity correction using a 30 million count Tc-99m flood, or Ga-67 flood. Attenuation corrections do not appear to improve the images. Transaxial reconstructions are performed using the Ramp Hanning filter with no cut-off, followed by a non-linear 3D filter of the transaxial reconstruction. Sagittal and coronary reconstructed images are then obtained.

THE IMPORTANCE OF SPECT FOR RADIOIMMUNO DIAGNOSTIC IMAGING - USING LABELED MONOCLONAL ANTIBODIES

Monoclonal antibodies have been labeled with I-131 and In-111. Labeling with Tc-99m is being developed and will probably come to clinical fruition in the not too distant future. In order to compare the thresholds of visualization of radioisotope concentrating lesions in a thorax or abdomen phantom, we have performed a number of studies using In-111 and Tc-99m. The following results have been obtained:

1) Comparisons of planar and SPECT images of phantoms with In-111 activity levels equivalent to 500uCi doses as used in labeled leukocyte imaging, showed that for the same lesion to background count ratios and similar total imaging times, planar imaging detected smaller lesions than SPECT.

2) For higher adult dose equivalence of about 5mCi of In-111, (10 times the activity levels used in (1) above) similar to doses used in labeled monoclonal antibody tumor imaging, SPECT surpassed planar image capability for lesion visibility. This result dramatizes the importance of sensitivity for SPECT imaging.

3) For SPECT images two pixel thick slices gave slightly better information than one pixel thick slices.

4) Non-linear filter detected borderline lesions slightly better than linear filtered images, but linear filter gave "cleaner"

images.

5) Detectability of lesions was clearly superior for Tc-99m studies at equivalent adult dosages as used in the In-111 phantom studies. For example, when Tc-99m was used, a 1.2cm diameter lesion could be identified on SPECT images when lesion to background activity ratios were between 6.5 and 12-1. Using In-111, the same lesion required a 25-1 lesion to background activity ratio for detection by SPECT.

Patient studies have shown that SPECT gives considerably more detail about lesions than planar imaging. Because SPECT utilizes the scintillation camera imaging system to acquire image data from 360° around the object and the reconstruction into tomographic image slices can be viewed in multiple projections including coronal, sagittal, and transaxial views, SPECT makes available an image that does not have to be viewed from the perspective of a particular angle. The viewer can see behind an organ. Because the background can be separated from the target, the contrast of images is improved over available planar projection images. Anatomic localization and details of lesion extent are improved.

Sensitivity remains a major SPECT problem which can be solved using more detectors, redesigning collimators (fan beam collimators have sensitivity advantages), and foremost, by radiopharmaceutical development to use more optimal radionuclides

such as Tc-99m and other short-lived tracers.

STAGING LUNG CANCER; CORRELATIVE TECHNIQUES FOR EVALUATING MEDIASTINAL DISEASE

Since the introduction of mediastinoscopy in 1959 as a staging technique for evaluation of lung cancer, patients with spread of their tumor to mediastinal nodes have been spared the morbidity and mortality of the more invasive thoracotomy surgical procedure. However, in the process of saving the patients with inoperable lung cancer from a thoracotomy, those patients without spread to the mediastinal nodes now undergo two surgical procedures, the staging mediastinoscopy followed by the curative "thoracotomy" for diagnosis and therapy of lung cancer. Mediastinoscopy is however an invasive procedure that may result in various complictions and is of substantial financial cost as well. With that reasoning in mind, several studies have been undertaken to validate the accuracy of Ga imaging and CT mediastinal scans versus mediastinoscopy for evaluating mediastinal spread in lung cancer.

Gallium Imaging

Various studies have found that when the primary lung cancer concentrated Ga, imaging of the mediastinum for abnormal Ga

uptake revealed a true positive ratio for the Ga mediastinum scan (i.e., the ratio of the number of true positive Ga scans to the number of true positive mediastinoscopies) of 81-100% (4-7). The true negative ratio (i.e., the ratio of the number of true negative Ga scans to the number of true negative mediastinoscopies) varied between 53-86%. In our study, two patients were Ga positive, radiographically negative, and mediastinoscopy positive. We regard Ga imaging and chest roentgenography as complementary techniques. Although the chest roentgenogram is certainly a simpler, more readily available technique in patients with bronchogenic carcinoma, it cannot, by itself, be relied on in all patients to preselect which patients should undergo a mediastinoscopy.

Radiographic Tomography

The ability of roentgenographic techniques to detect mediastinal spread has been investigated by several groups. James and Ellwood (8) reported a 76% agreement between abnormal chest tomography and mediastinoscopy, and a 95% agreement between normal mediastinal tomography and negative biopsy. Acosta and Manfredi (9) found that the presence of either mediastinal node enlargement or a central primary lesion on the chest roentgenogram or tomograph was an important indication for mediastinal exploration. They concluded, however, that patients with "noncentral" lesions, defined as a mass separate from the hilum with linear extension that appeared to extend toward the

hilum on chest roentgenogram, did not warrant mediastinal exploration before thoracotomy.

Computed Tomography

Friedman et al (2), reported on a series of patients for whom surgical treatment of primary lung carcinoma was planned, chest films were supplemented with oblique views, esophagrams, gallium scans, and computed tomograms. Metastases were established pathologically in 32 mediastinal node regions in 19 different patients, in hilar nodes in three, and extra-nodally in two others. Chest films were abnormal in 12 of the 19 cases (37% false negative); supplementary views made no contribution. Gallium was taken up by the primary tumor in 15 cases and by mediastinal or hilar metastases in 12 (20% false negative). Computed tomography showed nodes >1cm in size in the biopsy-positive or adjacent mediastinal node region in 18 patients two readings, or one false negative in 19. The hilar and extra-nodal mediastinal metastases were all detected on CT. Though the false positive rate for CT scans with double reading was 38% of cases (28% of regions), it is a sensitive technique for screening for mediastinal involvement in patients who would otherwise require an invasive biopsy procedure before thoracotomy.

These results clearly support the use of CT scanning as a sensitive screening method for metastatic mediastinal node involvement in the staging of lung cancer. A false negative rate

of 1 in 19 cases or 1 in 32 regions (3-5%) is as good as the surgical biopsy procedure itself; indeed, the CT-missed node in this series and another had false negative frozen sections at surgery. Gallium scanning, with the method used in this study, had a high false negative rate (20%), though the results after exclusion of adenocarcinomas are more favorable: gallium missed only 1 of 11 cases with mediastinal or hilar metastases or invasion among these. Routine radiography had a high false negative rate in this series of partially selected patients of 7 of 19 cases (37%), and was not helped by the occasional supplementation of oblique views or esophagrams. Intrapulmonary (hilar) node involvement, not clinically the crucial issue, was recognized by CT in 9 of 10 proven cases, while radiography did very poorly (4 of 10 called positive), especially on the left (0 of 5).

REFERENCES:

1. Floch J, Alazraki N, Wooten W: SPECT and planar image detection of hot lesions in a chest phantom using Ga-67 and Tc-99m. J Nucl Med, Vol 25, No 5, p51, 1984
2. Friedman PJ, Feigin DS, Liston SE, Alazraki N, Haghighi P, Young JA, Peters RM: Sensitivity of chest radiography, computed tomography and gallium scanning to metastasis of lung carcinoma. Cancer 54:1300-1306, 1984
3. O'Donnell JK, Go RT, Feiglin DF, Mehta AC, Golish JA, MacIntyre WJ, O'Donovan PB, Ross JS, Emdur LI: Gallium-67 transaxial emission tomography in the staging of bronchogenic carcinoma. J Nucl Med 26:5, p75, 1985
4. Alazraki NP: Usefulness of gallium imaging in the evaluation of lung cancer. CRC Critical Reviews in Diagnostic Imaging, September 1980
5. Alazraki NP, Ramsdell JW, Taylor A, Friedman PJ, Peters RM, Tisi GM: Reliability of gallium scan and chest radiography compared to mediastinoscopy for evaluating mediastinal spread in lung cancer. Am Rev Respir Dis, 117(3), 415, 1978
6. Fosberg, RG, Hopkins GB, Kan MK: Evaluation of the mediastinum by gallium-67 scintigraphy in lung cancer. J Thorac Cardiovasc Surg 77(1), 76, 1979
7. DeMeester TR, Berkerman C, Joseph JG, Toscano MS, Golomb H, Bitran J, Gross NJ, Skinner DB: Gallium-67 scanning for carcinoma of the lung. J Thorac Cardiovasc Surg, 72(5), 699,

1976

8. James EC, Ellwood RA: Mediastinoscopy and mediastinal roentgenology, Ann Thorac Surg, 18, 531, 1974

9. Acosta JL, and Manfredi F: Selective mediastinoscopy, Chest 71, 150, 1977.

NOTES

SPECT IN CLINICAL PRACTICE

Orthopedic Applications of SPECT Imaging

B. David Collier, M.D.

When compared to planar bone scanning, single photon emission computed tomography (SPECT) has technical advantages of potential diagnostic significance. Planar imaging often superimposes substantial underlying or overlying activity on the bony structures of medical interest. SPECT, however, can be used to remove such unwanted activity. For example, in the hip the acetabulum extends downward behind the femoral head. Therefore, when using planar bone scanning techniques, the photon deficient defect typical of avascular necrosis (AVN) of the femoral head may be obscured by activity originating in the underlying acetabulum. By using SPECT, underlying and overlying distributions of activity can be separated into sequential tomographic planes. For this reason SPECT facilitates the detection of AVN of the femoral head (1,2).

Many bone structures suitable for SPECT imaging have not been studied in detail, and the potential of bone SPECT for

oncologic imaging has not been thoroughly investigated. However, clinical experience to date has shown a role for bone SPECT in examining patients with pain and dysfunction in the larger joints and bony structures such as the knees, hips, lumbar spine, and temporomandibular joints (TMJ).

The adult patients described below were injected intravenously with 25 mCi (925 MBq) of Tc-99m MDP three hours before imaging. The SPECT examinations were performed with a rotating gamma camera (G.E. 400T) equipped with a low-energy general-purpose collimator (64x64 matrix, 64 projections over 360 degrees, 20 seconds per projection). Following uniformity correction and a 9-point spatial smooth for each projection, SPECT images were reconstructed using filtered backprojection with a ramp filter. A linear map was most frequently used for displaying SPECT bone scintigrams. However, when searching for a photopenic defect in the femoral head at risk for AVN, a log map was preferred.

1. Knees. Twenty-seven patients with chronic knee pain were prospectively examined by conventional radiography and bone scanning with SPECT (3,4,5). When the results of subsequent arthroscopic examination of all 3 compartments of the knee were reviewed, bone SPECT was found to be the most sensitive non-invasive test for evaluating the extent of osteoarthritis.

Differences in detection sensitivity for articular cartilage damage and synovitis were greatest in the patellofemoral compartment where the 0.91 sensitivity of bone SPECT compared favorably with the results of planar bone imaging, conventional radiography, and clinical examination. Furthermore, both SPECT (1.00) and planar (0.91) bone scanning were highly sensitive indicators of chronic meniscus tears in a subgroup of 14 patients with the pre-arthroscopic clinical diagnosis of a torn meniscus. Results suggest that particularly when augmented with SPECT, bone scanning has potential as a high sensitivity screening examination in patients with osteoarthritis or other significant internal derangement of the knee.

2. Hips. Twenty-one patients with the clinical diagnosis of AVN of the femoral head were examined by conventional radiography and bone scanning with SPECT(6). A final diagnosis of AVN was established for 15 symptomatic patients with a total of 20 involved hips. SPECT and planar bone scintigraphy were considered positive for AVN only if a photopenic bony defect could be identified. Using bone SPECT, 17 of 20 hips (sensitivity of 0.85) were correctly identified whereas with planar imaging only 8 of 15 patients and 11 of 20 involved hips were detected. While 13 of 20 hips with AVN had radiographic abnormalities at the time of the initial bone scan, a subchondral

fracture -- the most specific radiographic finding of early femoral head AVN -- was present in only 6 instances. It is concluded that by identifying a photopenic defect that is nct evident on planar views, SPECT can contribute to the accurate diagnosis of AVN of the femoral head.

3. Lumbar Spine. Planar and SPECT bone scanning were compared in 19 adults with radiographic evidence of spondylolysis and/or spondylolisthesis of the lumbar spine (7). SPECT was more sensitive than planar imaging when used to identify symptomatic patients and sites of "painful" defects in the pars interarticularis. Furthermore, SPECT allowed more accurate localization of abnormalities in the posterior neural arch. It is concluded that when spondylolysis or spondylolisthesis is the cause of low back pain, pars interarticularis defects frequently are associated with increased scintigraphic activity which is best detected and localized by SPECT.

4. Temporomandibular Joints. The diagnostic accuracy of conventional radiography, arthrography, and both SPECT and planar bone scanning were evaluated in 36 patients with TMJ dysfunction undergoing preoperative evaluation (8). The sensitivity of bone SPECT (0.94) was comparable to arthrography (0.96) and significantly better than planar bone scanning (0.76) or transcranial lateral radiography (0.04). While data for a larger asymptomatic control population are needed, preliminary results

give SPECT a diagnostic specificity of 0.70 for internal derangement of the TMJ requiring surgical correction. Lower sensitivity but comparable specificity for SPECT has been reported for series using arthrography rather than surgery to confirm the status of the TMJ (9,10). It is concluded that bone SPECT is a useful noninvasive imaging test to screen for internal derangement of the TMJ.

During the day-to-day operation of a busy nuclear medicine laboratory, the addition of SPECT to an orthopedic bone scanning procedure requires an extra 5 minutes for setup and patient positioning, 21 minutes for data acquisition, and 15 minutes for processing and filming. However, when examining patients with knee, hip, low back, and TMJ pain, SPECT bone scanning frequently gives images of greater clarity and in many instances provides unique diagnostic information. Specific advantages of SPECT in identifying and localizing skeletal pathology already have been established, and further diagnostic applications both for skeletal oncology and for the study of low back pain are anticipated.

REFERENCES

1. Collier BD, Johnson RP, Carrera G, Isitman AT, Hellman RS, Zielonka JS: Detection of avascular necrosis in adults by single photon emission computed tomography. J Nucl Med, 25:P25, 1984

2. Collier BD, Carrera GF, Johnson RP, Isitman AT, Hellman RS, Zielonka JS, Knobel J: Detection of femoral head avascular necrosis in adults by SPECT. J Nucl Med 26:979-987, 1985

3. Collier BD, Johnson RP, Carrera GF, et al: Single photon emission computed tomography in suspected internal derangements of the knee. J Nucl Med 24:P41, 1983

4. Collier BD, Johnson RP, Carrera GF, et al: Use of bone scintigraphy as a screening examination for torn menisci

in patients with chronic knee pain. Radiology 153:p212, 1984

5. Collier BD, Johnson RP, Carrera GF, et al: Chronic knee pain assessed by SPECT: Comparison with other modalities. Radiology 157:795-802, 1985

6. Collier BD, Johnson RP, Carrera G, et al: Detection of avascular necrosis in adults by single photon emission computed tomography. J Nucl Med 25:P25, 1984

7. Collier BD, Johnson RP, Carrera GF, et al: Painful spondylolysis or spondylolisthesis studied by radiology and single-photon emission computed tomography. Radiology 154:207-211, 1985

8. Collier BD, Carrera GF, Messer EM, et al: Internal derangement of the temporomandibular joint: Detection by single-photon emission computed

tomography. Radiology 149:557-561, 1983

9. O'Mara RE, Katzberg RW, Weber DA, et al: Skeletal imaging and SPECT in temporomandibular joint disease. Radioloy 101:p101, 1983

10. Katzberg RW, O'Mara RE, Tallents RH: Radionuclide skeletal imaging and single photon emission computed tomography in suspected internal derangements of the temporomandibular joint. J Oral Maxillofac Surg 42:782-787, 1984

NOTES

SPECT IN CLINICAL PRACTICE

SPECT Studies of the Heart

Harvey J. Berger, M.D.

Introduction

Thallium-201, the current radionuclide of choice for myocardial perfusion imaging, is rapidly extracted from the blood by the myocardium in a fashion analogous to potassium. This transport is mediated by the sodium-potassium ATPase pump. Thallium is distributed according to regional myocardial blood flow and is extracted by the myocardial cells rapidly. Maximal thallium-201 uptake occurs in peak exercise. Thereafter, intracellular thallium-201 equilibrates with the whole body thallium pool, and washout of thallium occurs. In the presence of coronary artery obstruction, the myocardium supplied by the stenotic vessel may be under perfused at peak exercise, and thallium-201 accumulation may be reduced and/or delayed. Likewise, thallium-201 washout may be slower, and there may be relative regional accumulation of thallium-201 in the ischemic zone.

During the past 10 years, there has been widespread utilization of exercise planar thallium-201 imaging to evaluate regional myocardial perfusion. As a means of diagnosing corsonary artery disease, stress planar thallium-201 imaging has a relatively high sensitivity and specificity. The improved sensitivity of thallium-201 imaging over the conventional exercise electrocardiogram occcurs in part because imaging often will be positive when the electrocardiographic response cannot be interpreted or when inadequate levels of exercise do not lead to an ischemic end-point. The improved specificity of thallium-201 imaging occurs because the major cause of positive thallium-201 studies is coronary stenosis, whereas there are diverse causes for ST segment abnormalities with exercise other than myocardial ischemia. Functional assessment of coronary anatomy and severity of coronary artery disease represents a critically important application of myocardial perfusion imaging. Identification of left main or triple vessel coronary artery disease also has become important to patient selection for coronary angiography and revascularization.

In addition to the stratification between multiple vessel/left main disease and lesser types of stenoses, the individual location of coronary artery disease also is of clinical significance. For example,

patients with proximal left anterior descending coronary stenosis (and anteroseptal ischemia) have a higher morbidity than patients with single vessel involvement of either the right or left circumflex coronary arteries. Many studies have addressed the ability of exercise planar thallium-201 imaging to predict the site of individual coronary stenosis. The site of ST segment depression during exercise testing is a poor means of localizing coronary disease, while reversible thallium-201 defects are far more predictive. Especially using visual interpretation, planar exercise thallium-201 imaging is not sensitive enough to reliably detect individual coronary lesions. Prediction of left circumflex disease is the poorest, with a sensitivity of only approximately 40%. Furthermore, because of the frequent individual variation in areas perfused by the right coronary and left circumflex coronary arteries and their complex visualization on planar studies, it is extremely difficult to specify which vessel is involved based upon planar thallium-201 imaging. It must be remembered that qualitative thallium-201 imaging defines relative differences in perfusion between vascular beds. Therefore, it often only identifies the most severe defect and misses less pronounced areas of ischemia. This is one of the main reasons for its less than perfect sensitivity for the detection of individual coronary artery stenoses, but a far better overall accuracy for the presence or absence of coronary artery disease.

Thallium-201 myocardial perfusion imaging is usually more sensitive with increasing disease severity (higher sensitivity in triple vessel disease than in single vessel disease). It is more sensitive in the setting of greater than 90% luminal diameter narrowing than lesser degrees of coronary artery obstruction. One of the reasons for "false positive" thallium studies is the disparity between anatomic and physiologic stenosis. Abnormal regional myocardial perfusion has, in fact, been demonstrated in regions supplied by angiographically subcritical lesions (25-50% diameter narrowing). This would suggest that regional myocardial ischemia may occur in areas supplied by vessels not normally considered hemodynamically compromised based upon standard angiographic criteria. This issue has particular relevance in the followup of patients who have undergone revascularization procedures. For example, a patient with chest pain and a 40% diameter stenosis lesion with a significant trans-stenotic gradient clearly is a candidate for coronary angioplasty, and an appropriately localized perfusion defect should be considered a true positive.

Quantification of Planar Studies

Visual interpretation of exercise-redistribution planar thallium-201 images often is subject to substantial interobserver variability and is less than optimal for the evaluation of the extent of coronary artery disease. The visual method is particularly limited in detection of individual coronary lesions in patients with multiple vessel coronary artery disease and especially when the degree of stenosis in one

vessel is not severe. Because of these problems, quantitative techniques for analysis of regional thallium-201 distribution and washout have been developed. Since 1980, there has been extensive interest in quantification of thallium-201 uptake both spatially and temporally. This topic is discussed in depth in an accompanying article by Dr. Garcia and his colleagues. Myocardial profiles may be circumferential or linear and may assess either average or maximal activity at each point. Thus, a curve of myocardial counts at each location in the myocardial profile is obtained for exercise and redistribution activities and is expressed as a percentage. Quantitative analysis of thallium-201 studies affords a clinically relevant analysis of myocardial tracer kinetics which should allow identification of multiple ischemic zones not apparent from qualitative analysis alone. Recent studies have clearly demonstrated that the quantitative approach markedly improves the accuracy of thallium-201 imaging for determination of the location and extent of coronary disease. Abnormalities in thallium kinetics may be reflected in washout falling below a spatially derived absolute cutoff or as nonuniform regional washout exceeding the variability of washout in normals.

Alternative Forms of Stress

There are many clinical settings where, although exercise is difficult or impossible, assessment of coronary vascular reserve is desirable. The best alternative approach to dynamic exercise (treadmill or bicycle) involves maximal coronary artery vasodilatation using intravenous dipyridamole, which increases total myocardial blood flow in regions supplied by normal coronary arteries. This results in a relative myocardial perfusion defect in a vessel supplied by a stenotic coronary artery. Numerous studies have demonstrated that dipyridamole thallium-201 imaging is comparable to exercise thallium-201 imaging in terms of sensitivity and specificity and preferable in patients who cannot exercise, such as those with peripheral vascular disease. In addition, a recent study demonstrated the safety and usefulness of thallium-201 imaging after intravenous dipyridamole in patients recovering from acute myocardial infarction. This study showed that the technique was safe, even in this high risk group, and that the presence of reversible perfusion defects following infarction was a more sensitive predictor of subsequent cardiac events than the submaximal exercise tolerance test alone.

Although intravenous dipyridamole is not available commerically at this time in the United STates, it is anticipated that this agent will be available within the coming year. At this time, intravenous dipyridamole only is available on a physician sponsored Investigational New Drug Application. Dipyridamole is given at 0.141 mg per kg per minute for 4-5 minutes via an infusion pump. The patient's heart rate, blood pressure and electrocardiogram are monitored during the infusion. Following the dipyridamole infusion, many investigators suggest that the patient should

perform submaximal handgrip exercise (25% of maximal effort for 5 minutes) using the arm contralateral to that of the intravenous infusion. In either case, thallium-201 then is injected and imaging performed in a standard fashion. Aminophylline is a known antidote for dipyridamole and quickly reverses any of the pharmacologic effects of dipyridamole. A small percentage of patients develop headache, nausea, or dizziness, which can be ameliorated quickly by terminating the infusion and/or administering aminophylline.

Tomographic Thallium-201 Imaging

Routine planar thallium-201 imaging results in superimposition of myocardial regions. Small defects and/or multiple defects may be obscured because of overlap with normal regions. Furthermore, with a routine three view planar thallium-201 study, the entire myocardium is not visualized. It is for these reasons that single photon emission computed tomography was developed and applied to myocardial perfusion imaging. There is the potential for avoidance of such areas of regional overlap and thus accurate definition of multiple areas of regional ischemia.

Initially, thallium-201 tomography involved either seven pinhole or rotating slant hole collimators. Although these longitudinal tomographic techniques are somewhat more sensitive than analysis of unprocessed planar images, the major advantage of this form of acquisition probably was quantification and image enhancement, rather than tomography itself. A more truly tomographic approach utilizes a scintillation camera that rotates on a gantry and acquires images at frequent intervals about the circumference of the chest. With this method, a series of 32 or 64 planar images is obtained over at least a 180^{o} arc surrounding the heart. From these planar images, filtered backprojection techniques are utilized to generate transaxial tomographic slices. Data acquisition requires approximately 20-25 minutes, making the acquisition time comparable to that for a series of high resolution planar images. Recent studies utilizing visual interpretation of tomographic thallium-201 images have demonstrated a definite improvement in sensitivity, specificity, and accuracy compared with planar imaging. In fact, in one study, the presence of multiple coronary lesions was more accurately identified by tomography than by planar imaging.

Tomographic Methods

As with planar studies, exercise should be performed utilizing the Bruce treadmill protocol. Routine 12 lead electrocardiographic monitoring is performed. Exercise is continued until symptom limiting fatigue, greater than or equal to 3 mm ST segment depression, life threatening ventricular arrhythmias, or severe angina. Thallium-201 is injected at peak exercise approximately 45 seconds prior to termination of exercise. During the last 45 second period, exercise is continued, if

possible, at the peak level. In order to improve the counting statistics for the tomographic study, 3.5 mCi are utilized rather than the more conventional 2 mCi dose. Thallium-201 tomographic imaging begins within approximately 5 minutes of the termination of exercise. Electrocardiographic monitoring is continued during this time interval.

A rotating gamma scintillation camera (GE STARCAM 400 ACT) is utilized in our laboratory. Thirty-two individual planar views are obtained for 40 seconds per view over a 180^{o} arc. Data acquisition is a 64 x 64 format and begins at the 45^{o} right anterior oblique and continues through the 45^{o} left posterior oblique. Particular care should be taken to assure that the starting location is obtained reproducibly. This acquisition requires approximately 22 minutes. Redistribution images are obtained at approximately four hours after exercise using the identical acquisition parameters as described for exercise. In order to calculate thallium washout, the exact time interval between stress and delayed imaging is recorded. Patients are restricted to liquid intake during this period.

Acquisition of 128 or 64 views rather than 32 views, in our experience, does not improve the quality of tomographic thallium-201 images. Furthermore, based on the modulation transfer function of the camera system and the tomographic resolution for thallium-201, acquisition of 64 x 64 data should be sufficient for thallium-201 tomography. No aliasing would be expected. In addition, the statistics per pixel in 128 x 128 acquisitions are a factor of four less than for the 64 x 64 acquisitions. The 128 x 128 planar images are low in count rates, resulting in larger statistical fluctuations in the reconstructed data. Lastly, 180^{o} sampling is preferred over 360^{o} acquisition, because of the degradation of the images when the posterior 180^{o} data are included in the filtered backprojection. With the substantial attenuation of thallium-201 that occurs in the chest, especially from the posterior projections, 180^{o} acquisition is the preferred technique.

Quality control should include uniformity field flood correction, evaluation of the sinogram display (review of each projection), and correction for the center of rotation. Insufficient field flood statistics compared to the statistics acquired in patient data can cause ring artifacts in the tomographic reconstruction. A 30 million count cobalt flood is sufficient to correct thallium-201 data and to provide ring free reconstructions. Daily quality controls involves acquisition of a 3 million count flood and correction of this flood with the 30 million count flood to be sure that the detector is uniform and that all photomultiplier tubes are functioning correctly. The sinogram display, a two-dimensional distribution with bin projection on the x axis and view number on the y axis, is used to quality control the acquired planar data. Adequacy of planar views, including artifacts due to patient motion, can be detected through review of the sinogram display, as well as the rotating display of individual projections. Center of rotation

correction also is performed daily. Errors in determination of the center of rotation result in tuning fork artifacts, which may distort the observed uptake of thallium-201 in the myocardium. In addition, the unprocessed planar data are inspected using a rotating cine display to identify planar views out of the field of view, the presence of soft tissue attenuation artifacts (i.e. breast attenuation), and patient motion. After acquisition of the planar data, transaxial filtering is performed. A Ramp-Hanning filter which has a zero value at half the sampling frequency is applied to the 32 projections. This results in a series of transaxial tomograms. Thereafter, axial filtering (1-2-1) is applied in the direction perpendicular to the reconstructed slices. This assures that the reconstructed resolution is comparable in the x, y and z directions. Because the heart is oriented obliquely within the chest, with the apex more anterio. and lateral than the base, transaxial images transect the heart in a plane that is not parallel to the heart's long axis. Therefore, oblique angle "transcardiac" reconstructions are performed. This results in three data sets, specifically the short axis, the horizontal long axis (similar to the right anterior oblique), and the vertical long axis (similar to the left anterior oblique). A pair of perpendicular cursors are available on the image display superimposed on the horizontal long axis image. By moving either of these cursors, the operator can interrogate any of the short or long axis tomograms on the computer. Exercise and redistribution images can be compared directly on a slice by slice basis.

No attenuation correction is employed because an adequate method has not been found for thallium-201 data. Simulation studies have shown that assymetries observed in the uptake of thallium-201 in the walls of the myocardium can be explained by attenuation effects and the variations of reconstructed resolution with depth. However, until a better method for attenuation correction has been derived, these attenuation effects need to be considered in image interpretation and in comparisons with normal data files.

Quantification of Tomographic Data

After a generation of standard orthogonal cardiac images, a bullseye polar coordinate map is derived. This method compresses the data from an entire tomographic study into a single quantitative functional image. Each of the short axis tomographic slices from apex to base is divided into 40 equal sections (9^{o} each); the maximal number of counts per pixel within each sector then is determined. These 40 values are plotted as a circumferential profile of the maximal counts per pixel versus angular sector location. A similar profile is constructed for each slice and to take into account variations for heart size and number of slices per study, these curves are interpolated to produce a total of 15 profiles. Each of the rectangular coordinate profiles is translated into a polar coordinate profile, which displays the same curve as a circle composed of 40 individual pixels. The data then are displayed as

a series of 15 concentric circles with the apex at the center and the base at the periphery. This analysis is performed on both the stress and delayed data sets and on the calculated thallium-201 washout. To correct the acquired data to a precise four hour interval between stress and delayed imaging, monoexpoential washout of thallium-201 is assumed.

Stress and redistribution thallium-201 studies are analyzed independently using both interpretation of the oblique angle slices and the bullseye polar coordinate map.

Definition of Normal Thallium-201 Distribution and Sources of Error

From analysis of a group of patients with a low probability (less than 5%) of coronary artery disease, the normal spatial distribution of thallium-201 at stress and redistribution was defined. These data were used to develop a gender-matched normal file for comparison against patients with coronary artsery disease. In a pilot study, each individual patient's bullseye was compared with a gender-matched normal file developed from this low probability of disease group. This resulted in the conversion of a bullseye display into a "standard deviation" map displaying pixels that were 1, 2, 2.5, and 3 standard deviations below normal. These new quantitative images were compared to angiographic data which defined the presence and location of coronary stenoses. Based upon this analysis, we concluded that the best agreement between coronary angiography and thallium-201 imaging occurred when abnormal regions on the bullseye were defined as contiguous defects greater than 2.5 standard deviations below normal. Thereafter, a series of guidelines were developed to assign a perfusion defect to a specific coronary artery. Furthermore, evaluation of the normal group demonstrated that the distribution of thallium-201 in the myocardium was heterogeneous. For example, the septum had less activity than the posterolateral wall, both in males and females. The apex always had less activity than the surrounding walls. In females, there was a decrease in activity in the inferior wall, but this was not apparent in the males. These variations in the distribution of thallium-201 are taken into account when analyzing individual oblique angle slices and when comparing the patient's bullseye to normal files. Reversibility consistent with myocardial ischemia also is defined from both the oblique angle slices and the bullseyes. Redistribution was considered present when the size of the defect decreased and/or when the severity of the defect diminished, that is, changed from greater than 2.5 to 1 standard deviation below normal. This method also allows differentiation of myocardial infarction (scar) from reversible myocardial ischemia.

Particular care must be taken in the evaluation of the reconstructed slices to identify soft tissue or breast attenuation artifacts, motion artifacts, poor count images, or falsely slow washout. For example, motion in a single tomographic slice can result in false positive defects. Furthermore, low count rates can result in images that

are difficult to interpret and, in fact, may have a "bizarre" appearance. If thallium-201 washout is evaluated, it is essential to determine whether or not there is evidence of dose infiltration. If a dose is even partially infiltrated, then thallium-201 washout from the heart will be spuriously delayed. In our laboratory, we routinely obtain images of the injection site and the contralateral site to assure that dose infiltration has not occurred.

Clinical Validation

A prospective group comprising 210 patients with coronary artery disease was evaluated in a totally blinded fashion. Of these patients, 93 had single vessel disease, 73 had two vessel disease, and 13 three vessel disease. Thirty-one of the patients were normal or had subcritical coronary lesions (less than 50% diameter stenosis). Each coronary artery lesion was measured in multiple projections using digital electronic calipers without any knowledge of the thallium-201 studies. The final diameter stenosis was expressed as the mean of these measurements. From this prospective group, the overal sensitivity for detecting the presence or absence of disease was 94% (176/187 patients) and the specificity was 91% (21/23). In the analysis of individual coronary artery stenoses, a perfusion defect was classified as true positive only if it was present in the anatomically correct region of the bullseye. The overall sensitivity for correctly identifying individual coronary stenoses was 80%, with a specificity of 93%, giving a diagnostic accuracy of 86%. On a vessel by vessel basis, the data were as follows:

	Coronary Stenosis			
	LAD	LCX	RCA	LCX/RCA
+ Predictive Value	80%	89%	87%	92%
- Predictive Value	82%	82%	89%	82%

It is of interest that 23 of the 36 "false positives" in the entire group occurred because of perfusion defects in a region supplied by a subcritical coronary lesion (40-50%). Thus, it appears that this technique is highly accurate for detecting coronary artery stenoses, and in fact, appears very sensitive for detecting subcritical coronary lesions. These results agree with the preliminary studies of Tamaki et al and Garcia et al who also have shown that quantitative analysis of single photon emission computed tomography enhances the clinical utility and reproducibility of these methods. However, because of the lack of adequate correction for attenuation, scatter and object size, these techniques as of yet do not allow extraction of absolute myocardial thallium-201 concentration.

Future Directions

Although thallium-201 is the radionuclide of choice at this time, extensive research is ongoing to develop a technetium-99m replacement. The most encouraging work involves technetium-99m-butyl isonitrile (TBI) developed by Jones, Davison, and Holman. Excellent planar and tomographic images have been obtained with this new radiopharmaceutical in patients. More extensive clinical trials are getting underway. The availability of a clinically useful technetium-99m labeled agent for myocardial perfusion imaging should allow even better image quality. With a technetium-99m agent, it is likely that 360^{o} acquisition would be preferred over 180^{o}. In addition, correction for scatter, attenuation, and variable resolution should be more feasible. This also should be the impetus for development and evaluation of multidetector camera systems including dedicated ring detectors. Elliptical orbit tomography in which the detector is kept close to the thorax is another technique that is presently undergoing evaluation. This approach should provide both better resolution and sensitivity and may improve thallium-201 data.

It is likely that with the enthusiasm for tomographic thallium-201 imaging and quantitative analysis that this will represent a major area of growth in nuclear medicine in the coming years. This should allow us to reach our goal of noninvasive detection and quantification of coronary artery disease.

Selected References

1. Zaret BL, Batler A, Berger HJ, et al: Nuclear Cardiology: Report of International Society and Federation of Cardiology and World Health Organization Task Force. Circulation 70:768A-781A, 1984.

2. Berger HJ and Zaret B: Nuclear Cardiology. Medical Progress. N. Engl. J. Med. 305:799-807 and 855-865, 1981.

3. Zaret BL, Strauss HW, Martin ND, et al: Noninvasive Regional Myocardial Perfusion with Radioactive Potassium: Study of Patients at Rest, Exercise and During Angina Pectoris. N. Engl. J. Med. 288:809, 1973.

4. Okada RD, Boucher CA, Strauss HW, et al: Exercise Radionuclide Imaging Approaches to Coronary Artery Disease. Am. J. Cardiol. 46:1188-1201, 1980.

5. Verani MS, Marcus ML, Razzak MA, et al: Sensitivity and Specificity of 201-Tl Perfusion Scintigrams Under Exercise in the Diagnosis of Coronary Artery Disease. J. Nucl. Med. 19:773, 1978.

6. Botvinick EH, Taradash MR, Shames DM, et al: Thallium-201 Myocardial Perfusion Scintigraphy for the Clinical Clarification of Normal, Abnormal, and Equivocal Electrocardiographic Stress Tests. Am. J. Cardiol. 41:43-51, 1978.

7. Dunn RF, Freedman B, Bailey ID, et al: Localization of Coronary Artery Disease with Electrocardiography: Correlation with Thallium-201 Myocardial Perfusion Scanning. Am. J. Cardiol. 48:837-843, 1981.

8. Berman DS, Garcia EV, Maddahi J: Thallium-201 Myocardial Scintigraphy in the Detection and Evaluation of Coronary Artery Disease. In Clinical Nuclear Cardiology, Berman DS, and Mason DT (Eds). Grune and Stratton 1981, pp. 49-106.

9. Ritchie JL, Zaret BL, Strauss HW, et al: Myocardial Imaging with Thallium-201: Multicenter Study in Patients with Angina Pectoris or Acute Myocardial Infarction. Am. J. Cardiol. 42:345-350, 1978.

10. Watson DD, Campbell NP, Read EK, et al: Spatial and Temporal Quantitation of Planar Thallium Myocardial Images. J. Nucl. Med. 22:577-584, 1981.

11. Okada RD, Limy L, Rothendler J, et al: Split Dose Thallium-201 Dipyridamole Imaging: A New Technique for Obtaining Thallium Images Before and Immediately After Intervention. JACC 1:1302-1310, 1983.

12. Josephson MA, Brown BG, Hecht HS, et al: Non-invasive Detection and Localization of Coronary Stenoses in Patients: Comparison of Resting Dipyridamole and Exercise Thallium-201 Myocardial Perfusion Imaging. Am. Heart J. 103:1008-1018, 1982.

13. Leppo JA, O'Brien J, Rothendler JA, Getchell JD, and Lee VW: Dipyridamole Thallium-201 Scintigraphy in the Prediction of Future Cardiac Events After Acute Myocardial Infarction. N. Engl. J. Med. 310:1014-1018, 1984.

14. Tamaki N, Mukai T, and Ishii Y: Comparative Study of Thallium Emission Myocardial Tomography with 180° and 360° Data Collection. J. Nucl. Med. 23:661-666, 1982.

15. Nohara R, Kambara H, Suzuki Y, et al: Stress Scintigraphy Using Single-Photon Emission Computed Tomography in the Evaluation of Coronary Artery Disease. Am. J. Cardiol. 53:1250-1254, 1984.

16. Ritchie JL, Williams DL, Harp G, et al: Transaxial Tomography with Thallium-201 for Detecting Remote Myocardial Infarction. Am. J. Cardiol. 50:1236-1241, 1982.

17. Caldwell JH, Williams DL, Harp GD, et al: Quantitation of Size of Relative Myocardial Perfusion Defect by Single-Photon Emission Computed Tomography. Circulation 70:1048-1056, 1984.

18. Tamaki N, Yonekura Y, Muaki T, et al: Stress Thallium-201 Transaxial Emission Computed Tomography: Quantitative Versus Qualitative Analysis for Evaluation of Coronary Artery Disease. JACC 4:1213-1221, 1984.

19. Patterson RE, Horowitz SF, Eng C, et al: Can Exercise Electrocardiography and Thallium-201 Myocardial Imaging Exclude the Diagnosis of Coronary Artery Disease? Bayesian Analysis of the Limits of Exclusion and Indications for Coronary Angiography. Am. J. Cardiol. 49:1127-1135, 1982.

20. Patterson RE, Horowitz S, Eng C, et al: Can Noninvasive Tests Identify Patients with Left Main or Three Vessel Coronary Disease After a First Myocardial Infarction? Probability Analysis of Exercise Tests with Thallium-201 Imaging, Electrocardiography and Clinical Observations. Am. J. Cardiol. 51:361-372, 1982.

21. Maddahi J, Garcia EV, Berman DS, et al: Improved Non-Invasive Assessment of Coronary Artery Disease by Quantitative Analysis of Regional Stress Myocardial Distribution and Washout of Thallium-201. Circulation 64:924-935, 1981.

22. Garcia E, Maddahi J, Berman DS, et al: Space/time Quantitation of Thallium-201 Myocardial Scintigraphy. J. Nucl. Med. 22:309-317, 1981.

23. Garcia E, Van Train K, Maddahi J, et al: Quantification of Rotational Thallium-201 Myocardial Tomography. J. Nucl. Med. 26:17-26, 1985.

24. DePasquale EE, DePuey EG, Nody A, et al: Accuracy of Quantitative Rotational Thallium-201 Tomography in Identifying Individual Coronary Stenoses: Use of Bullseye Functional Map. J. Nucl. Med. 26:5, 1985.

25. DePuey EG, Nody A, DePasquale E, et al: Abnormal Thallium-201 Tomographic Studies Early After Coronary Angioplasty (PTCA): Pathophysiologic Implications. Submitted for Publication.

26. DePuey EG, DePasquale E, Nody A, et al: Sequential Multivessel Coronary Angioplasty Assessed by Thallium-201 Tomography. Submitted for Publication.

27. Holman BL, Jones AG, Lister-James J, et al: A New Tc-99m-Labeled Myocardial Imaging Agent, Hexakist (t-Butylisonitrile)-Technetium(1)[Tc-99m TBI]: Initial Experience in the Human. J. Nucl. Med. 25:1350-1355, 1984.

NOTES

SPECT IN CLINICAL PRACTICE

SPECT-Tl-201 Cardiac Imaging

Daniel S. Berman, M.D.

A. LIMITATIONS OF PLANAR THALLIUM-201 IMAGING

B. TOMOGRAPHIC ACQUISITION PROTOCOL

C. QUANTITATIVE ANALYSIS
   1. Slice Selection
   2. Circumferential Profile Generation
   3. Comparison to Normal Limits
   4. Polar Display of Results

D. SENSITIVITY & SPECIFICITY

E. SOURCES OF ERROR
   1. Patient Motion
   2. Upward Creep

F. CLINICAL APPLICATIONS

REFERENCES

1. Caldwell JH, Williams DL, Harp GD, Stratton JR, Ritchie JL: Quantitation of size of relative myocardial perfusion defect by single-photon emission computed tomography. Circulation 70:1048-1056, 1984

2. Garcia EV, Van Train K, Maddahi J, Prigent F, Friedman J, Areeda J, Waxman A, Berman DS: Quantification of rotational thallium-201 myocardial tomography. J Nucl Med 26:17-26, 1985

3. Prigent M, Maddahi J, Garcia E, Friedman J, Van Train K, Bietendorf J, Swan HJC, Berman DS: Thallium-201 stress-redistribution myocardial rotational tomography: Development of criteria for visual interpretation. Am Heart J 109:274-281, 1985

4. Prigent F, Maddahi J, Garcia E, Van Train K, Friedman J, Berman jD: Noninvasive quantification of the extent of jeopardized myocardium in patients with single-vessel coronary disease by stress thallium-201 single-photon emission computerized rotational tomography. Am Heart J 111:578-586, 1986

5. Tamaki N, Yonekura Y, Mukai T, Kodama S, Kadota K, Kambara H, Kawai C, Torizuka K: Stress thallium-201 transaxial emission computed tomography: Quantitative versus qualitative analysis for evaluation of coronary artery disease. J Am Coll Cardiol 4:1213-1221, 1984

6. Friedman J, Garcia B, Berman D, Bietendorf J, Prigent F, Van Train K, Waxman A, Maddahi J: Motion selection and correction in Tl-201 SPECT imaging: A simple, practical method. J Nucl Med 25:P70, 1984

7. Maddahi J, Prigent F, Staniloff H, Garcia E, Becerra A, Van Train K, Swan HJC, Waxman A, Berman D: Quantitative interpretation of myocardial Tl-201 single photon emission computerized tomography: A probabilistic approach to the assessment of coronary artery disease. J Nucl Med 26:P60, 1985

8. Maddahi J, Van Train K, Wong C, Prigent F, Gurewitz J, Friedman J, Berman D: Quantitative analysis of Tl-201 myocardial single-photon emission computerized rotational tomography: Development, validation, and prospective application of an optimized computer method. J Am Coll Cardiol 7:22A, 1986

9. Friedman J, Van Train K, Maddahi J,Hasegawa B, Bietendorf J, Waxman A, Berman D: "Upward creep" of the heart: A frequent source of false-positive reversible defects on Tl-201 stress-redistribution SPECT. J Nucl Med 27:899, 1986

10. Prigent F, Maddahi J, Berman DS: Quantitative stress-redistribution Tl-201 single-photon emission tomography (SPECT): Development of a scheme for localization of coronary artery disease. J Nucl Med 27:997, 1986

11. Maddahi J, Van Train KF, Wong C, Gurewitz J, Prigent F, Youngkin C, Friedman J, Berman D: Comparison of Tl-201 single photon emission computerized tomography (SPECT) and planar imaging for evaluation of coronary artery disease. J Nucl Med 27:999, 1986

NOTES

SPECT IN CLINICAL PRACTICE

Organ Imaging

Summation

Barbara Y. Croft, Ph.D.

NOTES